SWELLING OF POLYMER GELS

by

Jaspreet Singh

Department of Chemical Engineering
McGill University
Montreal, Quebec
Canada

November 1993

A Thesis Submitted to the Faculty of Graduate Studies and Research
In Partial Fulfillment of the Requirements
For the Degree of
Master of Engineering

in fond memory of my grandparents
Harbans Kaur and Awtar Singh

"[T]he diffusion ... is left completely to the influence of the molecular forces basic to the same law...for the spreading of warmth in a conductor and which has already been applied with great success to the spreading of electricity"

Adolf E. Fick

in *Poggendorff's Annelen der Physik*, **94**, 59 (1855)

Abstract

The swelling equilibrium and kinetics of weakly crosslinked, non-ionic poly(N-isopropylacrylamide) gels were studied in water at a constant temperature of 298 K. The gel structure was varied by changing the monomer concentration, the proportion of crosslinker, and the temperature at gel formation. The relationship between the fractional approach to equilibrium (F) and the square root of time ($\sqrt{t}$) was sigmoidal

A model was developed to describe the kinetics of gel volume change for swelling or collapse The model was based on Fick's first law and accounted for the movement of the boundary of the gel. Numerical computations for one-dimensional cases involving planar, cylindrical and spherical geometries were performed with a constant diffusion coefficient Experimental data for disk-shaped and spherical poly(NIPA) gels in water and for spheres of rubber in toluene were well fitted by the model using a constant mutual diffusion coefficient Composition dependent mutual diffusion coefficients including those suggested by the scaling theory, also gave good agreement with experiments A new categorization of diffusion in polymers based on the F versus $\sqrt{t}$ plot is proposed.

Résumé

Nous avons étudié l'équilibre et la cinétique du gonflement des gels poly(N-isopropylacrylamide) non-ioniques et faiblement réticulés, dans l'eau à une température constante de 298 K. Nous avons varié la structure du gel en changeant la concentration du monomère, la proportion des liens et la température de gélation La relation entre l'approche fractionnaire à l'équilibre (F) et la racine carrée du temps ($\sqrt{t}$) s'est avérée sigmoïdale.

Nous avons développé un modèle pour décrire la cinétique du changement de volume du gel lors du gonflement et du dégonflement. Ce modèle est basé sur la première loi de Fick et tient compte du mouvement des frontiéres du gel Des évaluations numériques pour les cas unidimensionnels impliquant les géométries planaire, cylindrique et sphérique ont été réalisées avec un coéfficient de diffusion constant. Les données expérimentales pour les gels poly(NIPA) à forme de disque -dans l'eau- et pour les sphères de caoutchouc -dans le toluène- se sont révélées en accord avec le modèle en utilisant un coéfficient de diffusion mutuel constant Les coéfficients de diffusion mutuels dépendant de la composition, y compris ceux suggérés par la théorie du "scaling", se sont également révélés en accord avec les expérimentations. Une nouvelle catégorisation de la diffusion des polymères basée sur F versus $\sqrt{t}$ est proposée.

Acknowledgments

To Professor Martin E Weber, for providing any number of suggestions to answer a single question and good criticism on both *representing* and *intervening*.

To Professor Juan H Vera, for his time and myriads of interesting comments and suggestions from a thermodynamic perspective

To Professors Alejandro D Rey and M. Hasan, for help with numerical computations.

To Dr Eric L Cheluget, for interesting discussions in our shared office and his rescuing guidance whenever I was stuck with a difficult problem

To Eric Hoffman of Concordia University for introducing me to the history and philosophy of science during our long Thursday night discussions at café Romolos.

To the past and present members of the research group for their suggestions and friendly cooperation in the lab

To the staff of Chemical Engineering, for all their efforts, especially to Anne Pirhoda, Pat Fong, Jéan Dumont, Bill Habib, Ed. Siliauskas, A Gagnon, Charles Dolan and Walter Greenland.

To the Department of Chemical Engineering for financial support.

To Dr Terry Maccagno, for critically reading the drafts and suggesting corrections.

To Arvinder P Singh, who kindly left his newly bought laser printer at my home, when it was most needed

To Christine Brabant and Veronique Germain, for their help in translating the abstract.

To all my good friends in Canada, U S , England and India who were a constant source of support, encouragement and skepticism.

To my parents, Mohini and Partap Singh, and my sister, Dilreen, for their tremendous love and affection and for their angelic patience.

Contents

List of Figures

List of Tables

List of Abbreviations

% C	Percentage crosslinker
% T	Total monomer concentration, *g/ml*
DEB	Deborah number
FSL	Fick's second law
GVC	Gel volume change
LCST	Lower critical solution temperature
MW	Molecular weight
NIPA	N-isopropylacrylamide

Nomenclature

Lower Case Letters

a_i	Activity of component i
f	Phenomenological friction coefficient
$\mathbf{j}_{iu^*}$	Diffusional flux of phase i, relative to reference velocity
k	Constant
$m(0)$	Mass of the penetrant sorbed at time zero
$m(t)$	Mass of the penetrant sorbed at time t
$m(\infty)$	Mass of penetrant sorbed at equilibrium
n	Number of data points
r	Eulerian coordinate (radial or cartesian)
r^o, r^*	Dimensionless radial coordinates
t	Time
u	Velocity of penetrating front
u_i	Velocity of phase i
u^*	Reference velocity
x	Cartesian material coordinate
x_i	Mole fraction of component i
x_o	Initial half thickness of slab
x_M	Maximum half thickness of slab

Upper Case Letters

B	Bulk modulus
D_c	Cooperative diffusion coefficient
D_m	Mutual diffusion coefficient

D_T	Thermodynamic diffusion coefficient
D_p	Polymer fixed diffusion coefficient
D_s	Solvent fixed diffusion coefficient
D_i^*	Self diffusion coefficient of phase i
D°, D^*	Fitted parameters
F	Fractional approach to equilibrium
$\mathbf{J}_i$	Volumetric flux density of phase i
K	Parameter of gel elasticity
M (0)	Mass of the gel at time zero
M (c)	Mass of the collapsed gel
M (d)	Mass of the gel
M (t)	Mass of gel at time t
M (∞)	Mass of gel at equilibrium
N_A	Avogadro's number
P	Pressure
R	Gas constant
R_o	Radius at time zero
R_p	Radius of equivalent dry polymer sphere or cylinder.
R(t)	Position of boundary at time t
S	Shear modulus
T	Absolute Temperature
T_g	Glass Transition Temperature
V	Specific volume

Greek Letters

α, β	Fitted parameters
ρ_i	Density of phase or component i
γ	Constant
χ	Polymer-solvent interaction parameter

δ	Characteristic dimension
μ_i	Chemical potential of component i
λ_m	Characteristic time of the fluid
$\lambda_1, \lambda_2, \lambda_1^*, \lambda_2^*$	Parameters
$\boldsymbol{\lambda}_1, \boldsymbol{\lambda}_2$	Parameters
Φ	Ratio of final to initial gel mass or volume Also, the ratio of initial to final polymer volume fractions.
φ_i	Volume fraction of phase i in the gel
φ_p^*	Normalized polymer volume fraction
φ_p^o	Polymer volume fraction at time zero
φ_p^{eq}	Polymer volume fraction at equilibrium
$\hat{\varphi}_p$	Instantaneous volumetric average polymer volume fraction
$\Delta\varphi_p$	Difference between equilibrium and initial polymer volume fraction
Π	Osmotic pressure
$\Re, \Re^*$	Objective function
τ_o	Dimensionless time based on R_o
τ_p	Dimensionless time based on R_p
θ_D	Characteristic time of the diffusion process
Θ_i	Mobility of component i

Subscripts

D	Diffusion
i	Dummy subscript
o	Initial
p	Polymer phase
s	Solvent phase

Superscripts

eq	Equilibrium
M	Maximum

CHAPTER 1

Introduction

Hydrogels, also known as *super-absorbents,* are used in infant diapers, the controlled release of drugs, artificial snow, urban flood control bags, non-drip frozen packaging, and fire extinguishing agents that remain solid after spraying (Brannon-Peppas *et al.,* 1990; Kudela, 1990) Some potential applications of hydrogels are in protein extraction, dry-farming, dewatering coal-fines, memory elements and as smart chemo-mechanical systems (Tanaka, 1981; Osada *et al.*, 1993) These materials may absorb from several times to several hundred times their own weight of water

What are gels ? It is easier to recognize gels than to define them. A gel may be considered as a forth state of matter intermediate between a solid and a liquid. Almdal *et al.* (1993) proposed that the term "gel" be limited to systems which have the following characteristics (a) they consist of two or more components, one of which is a liquid, present in substantial quantity and (b) they are soft, solid, or solid-like materials Thus sponges, foams, cotton, wood-pulp and xerogels (i e. dried gels) are not considered as gels The definition includes both *thermoreversible* (formed by physical junctions) and *thermoirreversible* (formed by chemical bonds) gels. Each category is further subdivided into polymer and non-polymer gels.

Hydrogels belong to the class of chemically crosslinked organic polymer gels. Such gels swell in good solvents, i e. solvents having affinity for the polymer, but do not dissolve. When the good solvent is water, the gel is called a hydrogel. The properties of the gel depend strongly on the interaction of the polymer matrix and the solvent. The liquid prevents the polymer network from collapsing into a compact mass, and the network, in turn, retains the liquid. Hydrogels may be crosslinked by covalent bonds, as in most synthetic gels, or by Van der Waal's forces and hydrogen bonds

Synthetic hydrogels can be made by polymerization or copolymerization of hydrophilic monomer(s) with a crosslinking agent to produce homopolymer or co-polymer hydrogels, respectively When copolymerization is performed with an ionic or cationic monomer, the resulting gels are called anionic or cationic hydrogels, respectively. Classification of hydrogels can be made according to the chemical composition of the main monomer in the polymer network The degree of crosslinking and the amount of co-monomer are the major factors governing the properties of the resulting hydrogel. Polymer gels appear to be frozen systems (de-Gennes, 1979) in which the properties of the overall system during preparation and network formation determine the properties of the final system

Gel-gel phase transition: One remarkable property of certain hydrogels is that drastic changes in state can be brought about by small changes in external conditions The gel can swell and shrink discontinuously by as large as thousandfold (Tanaka, 1981; Illavsky *et al.*, 1982) by bringing about a continuous change in surrounding conditions such as temperature and solvent composition or, if the gel is ionic, salt concentration, pH and electric field. Such volume changes result in a dramatic changes in physical properties (Illavsky *et al.*, 1985; Tanaka, 1986; Vasheghani *et al*, 1992) For the temperature dependence of gel volume, three types of transitions have been reported: thermoswelling type (expansion with temperature), thermoshrinking type (contraction with temperature), and "convexo" type (a mixture of the other two types) Thermoswelling hydrogels contain mostly hydrophilic monomers, for example acrylamide, while thermoshrinking hydrogels are composed of monomers with hydrophobic substituents which make them less hydrophilic, e.g. N-isopropylacrylamide or NIPA

1.1. POLY(N-ISOPROPYLACRYLAMIDE) GELS

This work focuses on weakly-crosslinked non-ionic poly(N-isopropylacrylamide) gels [poly(NIPA)] In water, they undergo a discontinuous thermoshrinking volume phase transition. There is a parallel between the phase transition of poly(NIPA) gels and the phase separation of uncrosslinked poly(NIPA) in water, as illustrated in the following figure.

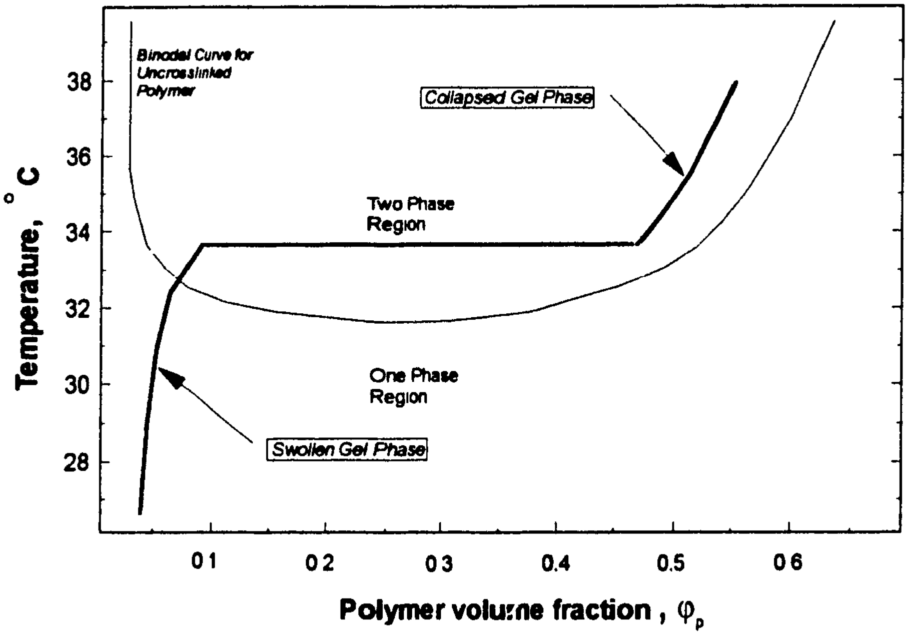

FIGURE 1.1. Gel-gel volume phase transition of poly(NIPA) gels and phase separation of uncrosslinked poly(NIPA) in water. [Heskins *et al.*, 1968 and Freitas *et al.*, 1987]

The minimum on the binodal curve for uncrosslinked polymer is a Lower Critical Solution Temperature (LCST) Below this temperature, 32°C, the polymer and water are completely miscible, but above it a two-phase region exists, consisting of a water rich phase and a polymer rich phase. The phase behavior of poly(NIPA) gels in water is similar, with a transition temperature of 34°C. Below this temperature the gel exists as macroscopically homogeneous and in highly swollen form, while above it the gel shrinks drastically by releasing water If poly(NIPA) gels are produced below the LCST, they are colorless and transparent, indicating good homogeneity If they are produced above the LCST, they are opaque, possibly due to the formation of micropores or other inhomogenieties Gehrke *et al.* (1991) found that the opaque gels formed above the LCST expanded 120 times faster and contracted 3000 times faster than comparable homogeneous gels formed below the LCST They hypothesized that this fast response is due to a bicontinuous interconnected porous structure arising from phase separation during gelation.

1.2. MODELS FOR GEL VOLUME CHANGE

The equilibrium aspects of gel volume have been extensively investigated Although accurate predictions of gel volume as a function of external conditions are not yet possible, a qualitative physical picture has been established On the other hand, the kinetics of volume change have received little attention.

From the thermodynamic viewpoint, the driving force for the transport of a substance relative to bulk flow arises from the gradient of its chemical potential This phenomenon is known as diffusion and can be formulated phenomenologically by application of the thermodynamics of the irreversible processes For a binary system at uniform temperature and pressure, the diffusional flux of component i is given by

$$\mathbf{j}_i = -D_T \nabla \mu_i \qquad [1.1]$$

where, μ_i is the chemical potential of component i and D_T is the thermodynamic diffusion coefficient In most cases, the chemical potential is unknown and Equation 1.1 is rewritten with the concentration gradient as the driving force.

$$\mathbf{j}_i = -D \nabla c_i \qquad [1.2]$$

where D, the diffusion coefficient, is generally concentration dependent (Crank, 1975).

Two types of models can be developed: molecular models and continuum models The molecular models aim to predict the diffusion coefficients, from information about the polymer network So far this approach has not produced accurate predictions of diffusion coefficients. The continuum models are used in conjunction with the experimental volume change data to estimate diffusion coefficients, which may then be related to the polymer composition of the gel. The latter approach is used in this thesis.

1.3. OBJECTIVES

1. To synthesize non-ionic poly(NIPA) gels using different gelation temperatures, monomer concentrations, and amounts of crosslinker;
2. To investigate the swelling kinetics of these hydrogels;
3. To formulate and test a model of the kinetics of swelling and collapse of hydrogels under isothermal conditions.

1.4. ORGANISATION OF THE THESIS

Chapter 2 outlines some general principles and definitions pertinent to the kinetics of gel volume change Various solvent transport mechanisms in polymers and gels are described along with a method to distinguish between them "Fickian" transport is critically examined. A moving boundary kinetic model is developed for highly swelling gels. Chapter 3 describes the procedures used for gel preparation, and reports the results of experiments involving gel swelling In Chapter 4, predictions are made using the model proposed in Chapter 2 for one-dimensional swelling and collapse in planar, cylindrical and spherical geometries. Diffusion coefficients are obtained by fitting the model to the experiments of Chapter 3 and other data available in the literature The composition dependence of the diffusion coefficients is compared to that suggested from theory. The conclusions of this study and recommendations for further work are presented in Chapter 5.

CHAPTER 2

Kinetics of Gel Volume Change: Theoretical Aspects

2.1. INTRODUCTION

According to Stannet *et al.* (1972), the sorption of small molecules by polymers has been studied for over 100 years, even before the macromolecular nature of polymers was recognized. See extensive reviews by Rogers (1965) and Frisch (1980). The solvent molecules not only penetrate into the polymer, but also swell it Thus the boundary between the liquid and the swelling polymer changes with time. The sorption of penetrant is also accompanied by bulk morphological changes and may result in phenomena such as swelling stress and cracking This work is concerned with free (as opposed to constrained) volume change of the *rubbery* polymer network

A polymer may exist in either of two states, namely, the rubbery state and the glassy state Above the glass transition temperature, T_g, a polymer is in the rubbery state, i e it is soft and elastic and can be easily deformed Below T_g, a polymer is in the glassy state stiff and hard and difficult to deform. A rubbery polymer readily changes its configuration in response to the stresses induced by penetrant molecules because thermal energy is available for doing so above T_g. Since glassy polymers deform with difficulty, their sorption behavior differs from that of rubbery polymers Sorption mechanisms in glassy polymers can be further complicated by the fact that the penetration of small molecules may cause a transition from the glassy to the rubbery state due to increased polymer chain mobility.

In this chapter various experimentally observed sorption types are discussed The semantics of various diffusion coefficients used in literature have been critically examined. The existing kinetic models are reviewed especially to locate reasons for the inability to deal with highly swelling gels. A better way to categorize the diffusion in polymers is proposed And finally a model is developed to describe the kinetics of gel volume change.

2.2. CHARACTERISTIC FEATURES OF SORPTION BEHAVIOR

Sorption is split into three broad divisions (Rogers, 1965):

[1] Fickian II Diffusion[1]

[2] Anomalous transport (Non Fickian Diffusion)

[3] Case II transport

There exists a general empirical equation to describe these different modes of transport They are usually distinguished by fitting sorption data over approximately the first half of the sorption curve, to the following equation (Fujita, 1968; Crank, 1975)

$$F = k(t)^n / \delta \qquad [2\ 1]$$

here, F is the fractional approach to equilibrium given by

$$F = \frac{m(t) - m(0)}{m(\infty) - m(0)} \qquad [2\ 2]$$

where

$m(0)$ = mass of the penetrant present at time 0.

$m(t)$ = mass of the penetrant sorbed at any time t.

$m(\infty)$ = mass of the penetrant sorbed at equilibrium.

---

[1] Commonly known as "Fickian" or "Case I" diffusion in the literature.

δ is the characteristic dimension of the gel at time zero; and, k and n are parameters. Table 2.1 lists the values of exponent n for various diffusion types. Representative swelling curves, fractional approach to equilibrium versus square root of time, for different diffusion types are shown in Figure 2.1.

TABLE 2.1. Exponent n of Equation 2.2 for various diffusion types:

Exponent n	Transport Type
0.5	Fickian II Diffusion
$0.5 < n < 1$	Anomalous (Non Fickian) Diffusion
1.0	Case II transport

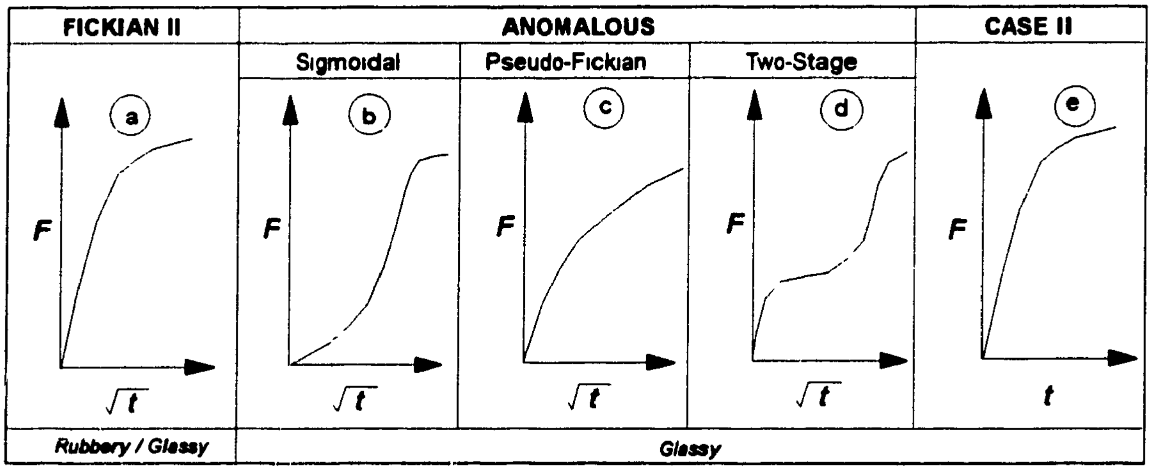

FIGURE 2.1. Swelling curves as indicators of transport types. Rogers (1965)

FICKIAN II TRANSPORT is characterized by a single parameter, the diffusion coefficient. The molecular relaxation in this case may be either much faster than diffusion ($T > T_g$) or extremely slow ($T < T_g$) and therefore not observed on the experimental time scale. A gel is regarded as Fickian II (see Figure 2.1.a) if it passes the following test

[1] The plot of F against $\sqrt{t}$ is linear in its initial portion (generally 40-60% of equilibrium).

[2] After the linear portion, the curve is concave to the $\sqrt{t}$ axis.

[3] The curves for different gel sizes (i.e. different δ values) superimpose on F versus $\sqrt{(t)}/\delta$.

ANOMALOUS TRANSPORT is generally observed below T_g and has been further categorized into three subclasses. These are sigmoidal, pseudo-Fickian, and two-stage behaviors (see Figure 2.1.b, c and d). The sigmoidal behavior of the sorption curve shows an inflection point around $F = 0\ 5$. Pseudo-Fickian sorption curves show a small linear region resembling Fickian II, but curves for different gel sizes do not coincide on the plot of F versus $\sqrt{\ t}/\delta$. The two-stage or dual mode of sorption is characterized by initial rapid uptake, establishment of a quasi-equilibrium, followed by a slow approach to final equilibrium.

CASE II TRANSPORT involves the motion of a boundary between a rubbery shell and a glassy core in the sample. This boundary moves at a constant velocity The weight gain is proportional to time (see Figure 2.1.e). Cases have also been reported where the mass transfer at the end of the sorption experiment is accelerated. This is usually referred to as super Case II transport.

Vrentas and Duda (1986) introduced a dimensionless group called the Deborah number, DEB, to characterize polymer-penetrant systems according to their diffusion behavior into one of the above categories.

$$(DEB)_D = \frac{\lambda_m}{\theta_D} \qquad [2.3]$$

where λ_m is the characteristic time of the fluid and θ_D is the characteristic time for the diffusion process. Table 2.2 shows the use of the Deborah number to anticipate the type of diffusional behavior.

TABLE 2.2. Classification of various diffusion types. *D* and *u* are the diffusion coefficient and the rubbery/glassy front velocity, respectively.

Deborah Number	Diffusion Type	Characteristics	Constitutive Equation	Rate Controlling Parameter	T
< 0.1	Fickian II	Molecular relaxation >> Diffusion transport	Classical Fick's Law	D	$> T_g$
≈ 1	Anomalous/Non-Fickian (*Pseudo-Fickian, Sigmoidal or Two-Stage*)	Molecular relaxation ≈ Diffusion transport	no general agreement	more than one	$< T_g$
≈ 1	Case-II	Molecular relaxation << Diffusion transport. (Relaxation at observable rates)	no general agreement	u	$< T_g$
> 10	Fickian II	Molecular relaxation << Diffusion transport	Classical Fick's Law	D	$\leq T_g$

2.3. THE DIFFERENCE BETWEEN FICKIAN I AND FICKIAN II TRANSPORT

The three characteristics of Fickian II, as mentioned in the previous section, are a direct consequence of the solution of Fick's second law with a fixed boundary (i.e. volume change is not taken into account). For small times (valid up to $F \approx 0.4$) these solutions are approximated by (Crank, 1975):

$$F = \gamma\sqrt{t/\delta^2} \qquad [2.4]$$

where γ is a constant, t is the time, and δ is either the initial thickness for a slab, or radius of a sphere or a cylinder. This result is valid for both a constant and a composition dependent mutual diffusion coefficient. Two points need to be clarified here.

For good solvents diffusing into polymers, the solvent molecules not only penetrate into the polymer but also swell it. Thus, the volume of the polymer changes with time, a factor not considered by the Fickian II treatment. Yet, in literature, the data obtained for swelling and collapse of gels, when found to be consistent with the three Fickian II characteristics are interpreted as a signature of Fickian II behavior, i e Fick's second law coupled with no volume change (Rogers, 1965).

Second, when the experimental F vs $\sqrt{t}$ curve is inconsistent with predictions based on Fick's second law without volume change, the anomalies are attributed to polymer relaxation: the finite rate of adjustment of polymer chains in the presence of the penetrant (Waksman *et al.*, 1990). Some investigators have attempted to explain these phenomena using the domain of linear irreversible thermodynamics Others, while severely criticizing this approach, have proposed a large scale revision of the diffusion laws According to Perez-Guerrero *et al.* (1991) the non-linear effects indicate the underlying phenomena occur in states which are far from local equilibrium, thus violating the fundamental assumption of the theory of linear irreversible thermodynamics. These conclusions overlook the fact that Fick's second law is the result of combining the species continuity equation with the constitutive equation for the diffusion flux (Fick's first law), under conditions where the volume average velocity is zero (Bird *et al.*, 1960). It is possible the diffusion flux to be described by Fick's first law and also to have a moving boundary such that Ficks second law does not apply. Such a situation is described in section 2.6.

It is proposed the transport should be called Fickian I if Fick's first law is valid and the boundary moves. Based on the evidence presented in Chapters 3 and 4, transport is regarded as Fickian I if the gel remains a rubber throughout the course of swelling or collapse and the following experimental features are observed:

[1] The plot of F against $\sqrt{t}$ is linear or sigmoidal in its initial portion (generally 40-60% of equilibrium).

[2] After the linear or sigmoidal portion, the F curve is concave to the square root of time axis.

[3] The curves for different size gels (i.e. with different δ values) superimpose on plots of F versus $\sqrt{t}/\delta$.

LINEAR FICKIAN I: Many rubbery polymer networks are known to absorb solvents, gases or vapors leading to minor swelling, with the ratio of final to initial equilibrium gel masses, Φ, close to 1. Some examples are rubber in benzene and polyethylene in water vapor (Rogers, 1965). An experimentally obtained initially linear swelling curve is illustrated in Figure 2.2.a. Such curves are usually denoted as Fickian II transport. However, the shape of the swelling curves and their overlap on F vs $\sqrt{t}/\delta$ are not unambiguous criteria for distinguishing Fickian II from Fickian I transport. Consider the identical looking Figures 2.2.a and 2.2.b. In such situations one needs to know whether the boundary moved to determine about the type of transport involved. If the boundary moves (i.e. volume changes) the transport is called linear Fickian I.

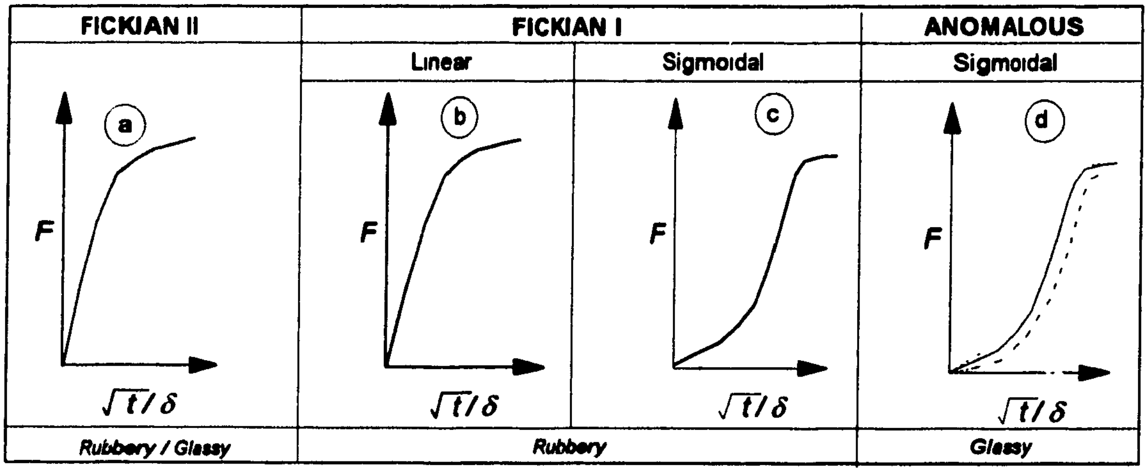

FIGURE 2.2. Swelling curves for Fickian I, Fickian II, and Anomalous transport.

SIGMOIDAL FICKIAN I: Weakly crosslinked organic polymers in the rubbery state, are known to absorb good solvents, leading to an appreciable change in volume (Φ values as large as 20). The swelling curves show a sigmoidal behavior Furthermore, curves for different values of the characteristic dimensions superimpose on a plot of F vs $\sqrt{t}/\delta$ (see Figure 2.2.c). Some examples include swelling of poly(NIPA) gels in water and rubber in toluene. This behavior will be called sigmoidal Fickian I, subsequently Often the sigmoidal swelling is taken as an indicator of "anomalous" or "non-Fickian" behavior (Waksman *et al.*, 1990). Some elastomers in the glassy state also show sigmoidal swelling behavior, but the swelling curves for different characteristic dimensions do not superimpose on F vs $\sqrt{t}/\delta$ (see Figure 2.2.d) Such cases are classified as anomalous

Figure 2.3 shows the commonly used classification of transport in polymers At the lowest level (inside the dotted rectangles) are the shapes of the experimentally determined swelling curves on F vs $\sqrt{t}$ or F vs t The linear and sigmoidal behaviors on F vs $\sqrt{t}$ are classified as Fickian II and Anomalous, respectively On the other hand, the linear behavior on F vs t is classified as Case II. This scheme does not account for any variants of Fick's first law other than Fickian II, does not take into account the swelling or collapse; and, does not justify the idea to categorize rubbery sigmoidal swelling along with glassy sigmoidal swelling, therefore, it needs to be modified A better way to categorize transport in polymers is proposed in Figure 2 4 The linear behavior on F vs $\sqrt{t}$ may be either Fickian I or Fickian II Similarly, the sigmoidal behavior may be either Fickian I or Anomalous A method to determine the transport type from the experimental data is proposed in Chapter 4

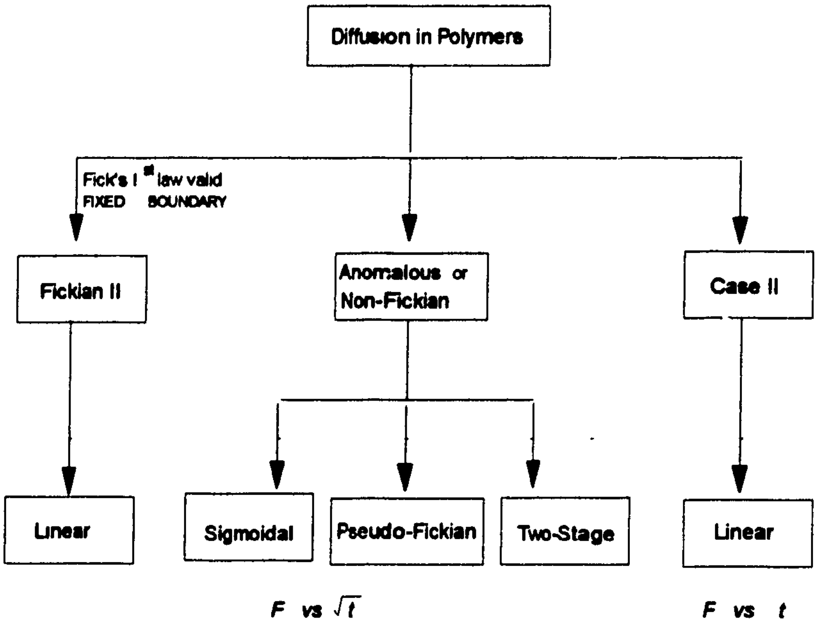

FIGURE 2.3. Present classification for diffusion in polymers.

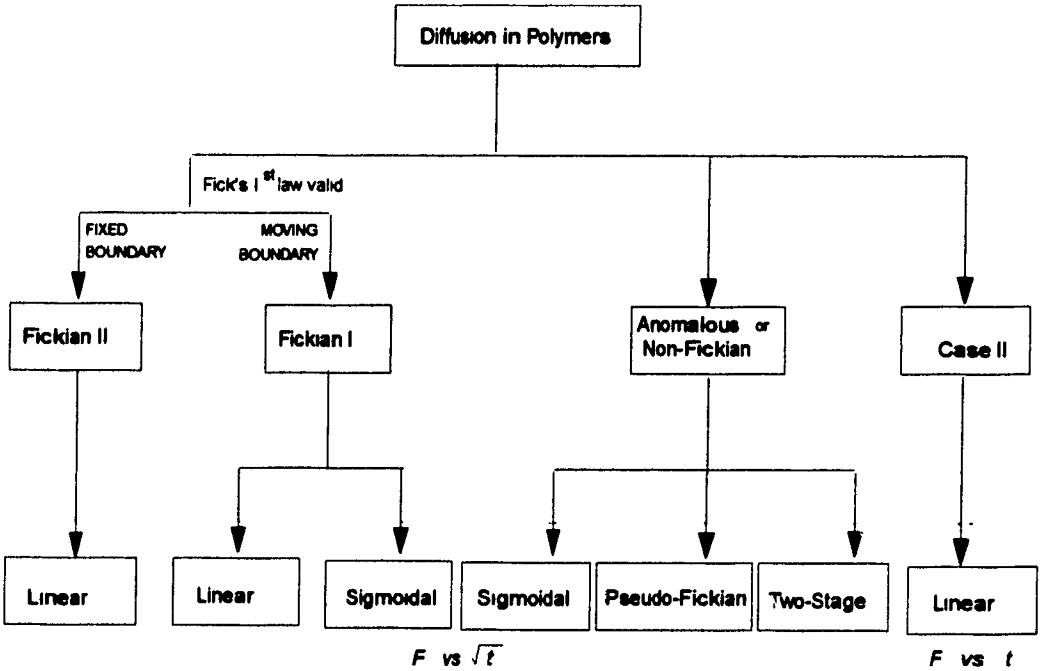

FIGURE 2.4. Proposed classification for diffusion in polymers.

2.4. DIFFUSION COEFFICIENTS

Descriptions of diffusion coefficients in polymers are available in the literature (Crank, 1975; Rogers, 1965; Vrentas, 1986). For a polymer-solvent system, there are six commonly used diffusion coefficients:

[1] mutual diffusion coefficient, D_m
[2] solvent fixed diffusion coefficient, D_s
[3] polymer fixed diffusion coefficient, D_p
[4] polymer self diffusion coefficient, D^*_p
[5] solvent self diffusion coefficient, D^*_s
[6] cooperative diffusion Coefficient, D_c

The first three, D_m, D_s and D_p, describe a diffusion process in a binary mixture or in a system composed of two single component phases (Vrentas, 1986). They are parameters of a binary system, and hence, not assignable to either the polymer or the solvent component (phase). Usually, they vary with the polymer composition (volume fraction), temperature, and pressure, although the dependence on the pressure is weak. For a series of homologous polymers, the molecular weight becomes an additional parameter (Fujita, 1990).

The reference velocities for D_m, D_s and D_p and the relationships between these coefficients are given in the Table 2.3. The volumetric average velocity serves as the reference velocity for D_m , thus it is sometimes called the volume fixed diffusion coefficient The solvent-fixed diffusion coefficient, D_s, refers to the solvent velocity. The polymer velocity is chosen as the reference velocity for D_p. The three reference velocities are related by

$$\mathbf{u}_m = \varphi_s \mathbf{u}_s + \varphi_p \mathbf{u}_p \qquad [2.5]$$

TABLE 2.3. Relationship between the diffusion coefficients.

Reference velocity	Diffusion coefficient	Relationship with D_m
$\mathbf{u}_p$ Polymer velocity	D_p	$D_p = \left(\frac{D_m}{\varphi_p}\right)$
$\mathbf{u}_s$ Solvent velocity	D_s	$D_s = \left(\frac{D_m}{\varphi_s}\right)$
$\mathbf{u}_m$ Volume average velocity	D_m	-

The self diffusion coefficients, D^*_p and D^*_s, measure the mobility of the molecules, unlike the mutual diffusion coefficient which measures the rate at which concentration gradients disappear. D^*_p or D^*_s are determined by measuring the rate of diffusion of a small amount of radioactively tagged component (polymer or solvent) in a system composed of a uniform composition of untagged components (polymer and solvent). For a binary polymer-solvent solution there are two self diffusion coefficients (Vrentas, 1986):

$$D_p^* = RT\Theta_p = RT/f_p \qquad [2.6a]$$

$$D_s^* = RT\Theta_s = RT/f_s \qquad [2.6b]$$

where Θ_i is the mobility of component i and f_i is the friction coefficient which is the product of the effective viscosity of the medium and the effective diameter of component i. Most molecular theories derive expressions for D^*_i rather than D_m.

An approximate relationship between the self-diffusion coefficients and D_m, based on the combination of statistical mechanics with the phenomenological theory of irreversible processes, (Loflin *et al.*, 1969):

$$D_m = \left(\frac{\partial \ln a_s}{\partial \ln x_p}\right)_{T,p} \left[D^*_p x_p + D^*_s x_s\right] \qquad [2.7]$$

where a_s represents the activity of the solvent and x_i is the mole fraction.

Since the macromolecular D^*_p is generally much smaller than the small molecule D^*_s the above expression can be further simplified to the following form (Vrentas, 1986).

$$D_m = \frac{D^*_s \rho_p v_p \rho_s}{RT}\left(\frac{\partial \mu_s}{\partial \rho_s}\right) \qquad [2.8]$$

where μ_s is the solvent chemical potential per mole and v_p is the partial specific volume of the polymer. For the concentrated solution regime (i.e up to a solvent volume fraction of approximately 0.85) the above expression becomes

$$D_m = D^*_s Q \qquad [2.9]$$

where

$$Q = (1-\varphi_s)^2(1-2\chi\varphi_s) \qquad [2.10]$$

and χ is the polymer solvent interaction parameter from the Flory-Huggins polymer solution theory.

The cooperative diffusion coefficient, D_c describes the relaxation of fluctuations of the polymer concentration and the collective motion of polymer chains (Vrentas, 1986) It is measured by the quasi-elastic light scattering techniques. It has been shown experimentally that D_c approaches D_s for semi-dilute polymer solutions (Fujita, 1990) For good solvents, the scaling theory predicts (de-Gennes, 1979)

$$D_s \propto \varphi_p^{0.75} \qquad [2.11]$$

2.5. KINETIC MODELS: A LITERATURE SURVEY

Although several mathematical models of the kinetics of gel volume change have been formulated, so far a consistent treatment does not seem to have been given. The existing models can be split into three categories:

COLLECTIVE DIFFUSION MODELS

These models are based on the work done by Tanaka *et al.* (1973), who derived an equation of motion of the polymer network in a gel in order to describe light scattering by a hydrogel. Tanaka and Fillmore (1979) applied this equation of motion to the swelling process of spherical polyacrylamide and poly(NIPA) gels in water They treated the swelling of a gel as a process where a crosslinked network, initially under uniform stress, expands by osmotic pressure, sucking in the surrounding fluid. They criticized previous work, which they believed had incorrectly assumed that gel swelling was determined by diffusion of solvent molecules into the polymer network They proposed that the collective diffusion coefficient of the polymer network into water controls the swelling kinetics.

Peters and Candau (1986) generalized the Tanaka-Fillmore (TF) kinetic model by including the effect of the shear modulus. In 1990 Li and Tanaka formulated a new relation to extend the TF model to non-spherical gels. They predicted that the diffusion coefficients for a long cylinder and for a slab, respectively, 2.5 and 3.0 times smaller than that of a spherical gel Mazich *et al.* (1992) pointed out the flaws in the derivations of the TF model and its extended versions (where the divergence of a gradient was confused with the gradient of the divergence). Moreover, the models were tested only for volume changes between two highly swollen rubbery states containing more than 90 % water. In experiments with polyacrylamide gels the gel beads were not washed after preparation to remove impurities and unreacted monomers.

Komori and Sakamoto (1989) proposed an alternative to the TF model Their model involved a coupled diffusion equation for the excess concentration of penetrant with an expression for the distribution of local strain. No concentration dependence of the diffusion coefficient was assumed. Considerable discrepancies were found between the experimental results and the model predictions

NON-FICKIAN DIFFUSION MODELS

The models proposed by Berrens and Hopfenberg (1979) and further developed by Joshi and Astarita (1979) are inappropriate for rubbery swelling. Although these models were proposed to describe Non-Fickian behavior observed in *glassy* swelling, they have been widely used to account for sigmoidal swelling in rubbery gels (Waksman *et al.* 1990) These models are based on Fickian II diffusion and first order relaxation rate process and do not allow for the movement of the gel boundary The models involve three to six parameters, including the diffusion coefficient When swelling data are fitted by these models, the resulting diffusion coefficients may show unusual composition dependence, e.g. a maximum at an intermediate composition

FICKIAN DIFFUSION MODELS

These models make use of Fick's first law as the constitutive equation As discussed in Section 2.3, two different behaviors are possible Fickian I and Fickian II

Fickian II models (Buckley *et al* 1962) are inappropriate for rubbery gels because

[1] The model neglects the movement of the boundary caused by volume change.

[2] Even for a concentration-dependent diffusion coefficient the solvent uptake is initially proportional to the square root of time

Vasheghani-Farahani (1990) proposed a kinetic model using the chemical potential of the solvent as the driving force for the diffusion flux and accounting for boundary movement The chemical potential came from Flory-Huggins theory The swelling curves did not agree with experimental data, probably because of the limitations of the Flory-Huggins theory and the theory of rubber elasticity, which were used to obtain the chemical potential of the solvent.

Rossi *et al.* (1991) proposed a model based on the assumptions similar to those used in this work. They derived the governing equations only for one dimensional planar geometry, yet they tested the model (Mazich *et al.*, 1992) for a spheres

2.6. A MODEL FOR SWELLING OF POLYMER GELS

The mathematical model developed here incorporates volume changes due to penetrant swelling and allows for the concentration dependence of diffusivities The swelling process was modeled as isothermal two-phase motion of a polymer phase (p) and a low molecular weight solvent phase (s) Both phases are assumed to have constant and equal densities. The two continuity equations can be written

Polymer phase·

$$\frac{\partial \varphi_p}{\partial t} = -\nabla \mathbf{J}_p \qquad [2.12]$$

Solvent phase·

$$\frac{\partial \varphi_s}{\partial t} = -\nabla . \mathbf{J}_s \qquad [2.13]$$

where, φ_i is the volume fraction of phase i, $\mathbf{J}_i$ is the volumetric flux density (superficial velocity) of phase i with respect to the fixed coordinates, and t is the time. The volume fractions are constrained by

$$\varphi_p + \varphi_s = 1 \qquad [2.14]$$

Adding Equations 2.12 and 2.13

$$\nabla \left(\mathbf{J}_p + \mathbf{J}_s\right) = 0 \qquad [2.15]$$

Assuming that the solvent and polymer volumetric flux densities are zero at time zero, one gets

$$\mathbf{J}_p + \mathbf{J}_s = 0 \qquad [2.16]$$

The volumetric flux density is divided into two parts the diffusional flux and the convective flux. Let $\mathbf{j}_{su^*}$ be the volumetric flux density of the solvent relative to a reference velocity, $\mathbf{u}^*$. Then

$$\mathbf{J}_s = \mathbf{j}_{su^*} + \varphi_s \mathbf{u}^* \qquad [2.17]$$

Any reference velocity may be chosen, but the most common choices are the mass, molar, volume average, or the velocity of one of the phases.

If the volume average velocity, $\mathbf{u}_m$, is the reference velocity, the solvent volumetric flux density is

$$\mathbf{J}_s = \mathbf{j}_{su_m} + \varphi_s \mathbf{u}_m \qquad [2.18]$$

where

$$\mathbf{u}_m = \varphi_s \mathbf{u}_s + \varphi_p \mathbf{u}_p \qquad [2.19]$$

The velocities of the polymer phase and the solvent phase follow from the definitions of volumetric flux densities and volume fractions:

$$\mathbf{u}_p = \frac{\mathbf{J}_p}{\varphi_p} \qquad [2.20]$$

$$\mathbf{u}_s = \frac{\mathbf{J}_s}{\varphi_s} \qquad [2.21]$$

Using Equations 2.19, 2.20 and 2.21, Equation 2.18 can be reduced to the following form

$$\mathbf{J}_s = \mathbf{j}_{su_m} + \varphi_s \left(\mathbf{J}_p + \mathbf{J}_s\right) \qquad [2.22]$$

The description is completed by a constitutive equation, which defines the diffusion coefficient:

$$\mathbf{j}_{su_m} = -D_m \nabla \varphi_s \qquad [2.23]$$

where D_m is the mutual diffusion coefficient. Combination of equations 2.13, 2.14, 2.22 and 2.23, gives

$$\frac{\partial \varphi_p}{\partial t} = \nabla \left(D_m \nabla \varphi_p\right) \qquad [2.24]$$

which will be referred to as the *gel diffusion equation*, subsequently.

Combining Equations 2.14, 2.16, 2.20, and 2.22 gives

$$\mathbf{u}_p = -\frac{D_m}{\varphi_p} \nabla \varphi_p \qquad [2.25]$$

which will be referred to as the *interface equation*. This equation is used to obtain the velocity of the polymer at the gel/liquid interface.

Gel diffusion and interface equations can also be obtained by choosing the velocity of the polymer or the solvent as the reference velocity in Equation 2.17 and proceeding similarly. Table 2.4 presents the different forms. The equations are equivalent, since the three diffusion coefficients are related by

$$D_m = \varphi_p D_p = \varphi_s D_s \qquad [2.26]$$

TABLE 2.4. Different forms of gel diffusion and interface equations.

Reference velocity	Solvent volumetric flux density	Fick's first law	Gel diffusion equation	Interface equation
$\mathbf{u}_p$ Polymer velocity	$\mathbf{J}_s = \mathbf{j}_{su_p} + \varphi_s \mathbf{u}_p$	$\mathbf{j}_{su_p} = -D_p \nabla \varphi_s$	$\frac{\partial \varphi_p}{\partial t} = \nabla.\left(D_p\ \varphi_p \nabla \varphi_p\right)$	$\mathbf{u}_p = -D_p \nabla \varphi_p$
$\mathbf{u}_s$ Solvent velocity	$\mathbf{J}_s = -\mathbf{j}_{pu_s} - \varphi_p \mathbf{u}_s$	$\mathbf{j}_{pu_s} = -D_s \nabla \varphi_p$	$\frac{\partial \varphi_p}{\partial t} = \nabla.\left(D_s\ \varphi_p \nabla \varphi_p\right)$	$\mathbf{u}_p = -\frac{D_s\left(1-\varphi_p\right)}{\varphi_p} \nabla \varphi$
$\mathbf{u}_m$ Volume average velocity	$\mathbf{J}_s = \mathbf{j}_{su_m} + \varphi_s \mathbf{u}_m$	$\mathbf{j}_{su_m} = -D_m \nabla \varphi_s$	$\frac{\partial \varphi_p}{\partial t} = \nabla.\left(D_m \nabla \varphi_p\right)$	$\mathbf{u}_p = -\frac{D_m}{\varphi_p} \nabla \varphi_p$

2.7. GEL VOLUME CHANGE IN ONE DIMENSIONAL GEOMETRIES

For the one dimensional case, Equation 2.24 can be reduced

$$\frac{\partial \varphi_p}{\partial t} = \frac{1}{r^{\imath}}\left[\frac{\partial}{\partial r}\left(D_m\, r^{\imath}\, \frac{\partial \varphi_p}{\partial r}\right)\right] \qquad [2.27]$$

where $\imath = 0$, 1 and 2 for a slab, a cylinder and a sphere, respectively; r is the Eulerian spatial coordinate and t is the time.

The initial and boundary conditions are :

$$\varphi_p(r,0) = \varphi_p^{o} \qquad [2.28]$$

$$\varphi_p[R(t),t] = \varphi_p^{eq} \qquad \text{(for } t > 0\text{)} \qquad [2.29]$$

$$\left.\frac{\partial \varphi_p}{\partial r}\right|_{r=0} = 0 \qquad \text{(for } t \geq 0\text{)} \qquad [2.30]$$

where φ_p^{o} and φ_p^{eq} are the initial and equilibrium values of the polymer volume fraction in the gel. The quantity $R(t)$ is the half thickness for a slab and the radius for a cylinder or a sphere.

It is assumed that at the boundary between the swelling gel and the surrounding fluid, the equilibrium volume fraction is reached instantaneously. For one-dimensional geometry, the gel/liquid interface, located at $R(t)$, moves with the polymer velocity:

$$\frac{dR}{dt} = \left.\mathbf{u}_p\right|_{r=R(t)} \qquad [2.31]$$

Equation 2.25 yields the rate of change of $R(t)$ as

$$\frac{dR}{dt} = -\left.\frac{D_m}{\varphi_p}\frac{\partial \varphi_p}{\partial r}\right|_{r=R} \qquad [2.32]$$

Hence the model involves a time dependent *moving boundary*. The initial condition is

$$\text{at } t = 0 \qquad R(t) = R_o \qquad [2.33]$$

where R_o is the initial position of the boundary.

FRACTIONAL APPROACH TO EQUILIBRIUM

The fractional approach to equilibrium, F, is computed using the assumption that the densities of the polymer and solvent were equal.

$$F = \left(\frac{1}{\hat{\varphi}_p} - \frac{1}{\varphi_p^o}\right) \Big/ \left(\frac{1}{\varphi_p^{eq}} - \frac{1}{\varphi_p^o}\right) \qquad [2\ 34]$$

where φ_p^o is the initial polymer volume fraction, φ_p^{eq}, the final polymer volume fraction, and $\hat{\varphi}_p$ is defined as the instantaneous volumetric-average polymer volume fraction .

$$\hat{\varphi}_p(t) = \frac{i+1}{R^{i+1}} \int_0^{R(t)} \varphi_p(r,t)\,dr \qquad [2\ 35]$$

where i = *0, 1, 2,* for slabs, cylinders and spheres, respectively

2.8. COORDINATE TRANSFORMATION FOR THE SLAB GEOMETRY

The coordinates may be transformed to recast Equations 2.27 to 2.33 from the Eulerian to the Langrangian or material coordinate form, thus fixing the position of the boundary. This transformation is successful only for the slab geometry ($i = 0$ in Eq 2.27)

Defining a new coordinate , *x* (*r*,*t*), such that

$$\left(\frac{\partial x}{\partial r}\right)_t = \varphi_p \qquad [2.36]$$

and using it along with the definition of the polymer velocity

$$\left(\frac{\partial r}{\partial t}\right)_x = \mathbf{u}_p \qquad [2.37]$$

one arrives at the following transformed coordinate form of Equation 2.27 for planar geometry with a constant D_m

$$\frac{\partial \varphi_p}{\partial t} = D_m\, \varphi_p^2 \frac{\partial^2 \varphi_p}{\partial x^2} \qquad [2.38]$$

In case D_m is composition dependent, Equation 2.27 reduces to

$$\frac{\partial \varphi_p}{\partial t} = \varphi_p^2 \left[D_m(\varphi_p) \frac{\partial^2 \varphi_p}{\partial x^2} + \frac{\partial D_m(\varphi_p)}{\partial \varphi_p} \left(\frac{\partial \varphi_p}{\partial x} \right)^2 \right] \qquad [2.39]$$

See Appendix I for the detailed derivations. The initial and boundary conditions for both cases are

$$\varphi_p(x,0) = \varphi_p^{\circ} \qquad [2.40]$$

$$\varphi_p(x_M, t) = \varphi_p^{eq} \qquad (\text{for } t > 0) \qquad [2.41]$$

$$\left.\frac{\partial \varphi_p}{\partial r}\right|_{x=0} = 0 \qquad (\text{for } t \geq 0) \qquad [2.42]$$

here the gel/liquid interface is fixed at

$$x_M = \int_0^{R(0)} \varphi_p^{\circ}\, dr \qquad [2.43]$$

CHAPTER 3

Experimental: Gel Synthesis, Swelling and Analysis of Results

3.1. INTRODUCTION

The present work was primarily with the kinetics of swelling of weakly crosslinked, highly swelling poly(NIPA) gels over a large range of concentration. The variables studied included the total monomer content, the temperature at gel formation, the degree of crosslinking, and the gel thickness.

3.2. DEFINITIONS

GEL COMPOSITION:

The gel composition was specified by the relative amount of monomer(s) and solvent (water) at preparation The following variables are convenient for defining the gel composition (Vasheghani-Farahani, 1990):

$$\%T = \frac{\text{mass of all monomers (g)}}{\text{volume of solution (ml)}} \times 100 \qquad [3.1a]$$

$$\%C = \frac{\text{mass of crosslinker (g)}}{\text{mass of all monomers (g)}} \times 100 \qquad [3.1b]$$

FRACTIONAL APPROACH TO EQUILIBRIUM:

The fractional approach to equilibrium, $F(t)$, was calculated from

$$F = \frac{M(t) - M(0)}{M(\infty) - M(0)} \qquad [3.2]$$

where

$M(t) \equiv$ Mass of gel at time t;

$M(0) \equiv$ Initial mass of gel $(t = 0)$;

$M(\infty) \equiv$ Final mass of gel $(t \to \infty)$;

Equilibrium Mass Ratio (Φ):

The equilibrium mass ratio of the gels was defined as

$$\Phi = \frac{M(\infty)}{M(0)} \qquad [3.3a]$$

For constant and equal densities of the solvent and the polymer phases, the above is the same as equilibrium volume ratio

$$\Phi = \frac{V(\infty)}{V(0)} \qquad [3.3b]$$

where $V(\infty)$ and $V(0)$ are the final and initial volumes of the gel, respectively.

3.3. GEL PREPARATION

Gels were prepared by free radical polymerization of N-isopropylacrylamide in an aqueous solution, using N,N$'$- methylenebisacrylamide as the crosslinking agent. All chemicals were reagent grade and were used without further purification. They were purchased from Pfaltz and Bauer (USA). Polymerization was initiated using the redox couple of ammonium persulfate with sodium metabisulfite (see Table 3.1 and Figure 3.1).

The procedure was the following: The weighed monomer and 100 ml of degassed and deionized water were transferred to a nitrogen filled glove-box. Forty ml of this water were placed in a 250 ml Erlenmeyer flask and the monomer and the cross-linking agent were dissolved in it Two initiator solutions were prepared with 15 ml of water, one containing 0.03g of ammonium persulfate and the other 0.03g of sodium metabisulfite. To begin the polymerization, 5 ml of each initiator solution were added to the monomer solution to make a total volume of 50 ml The resulting solution was mixed with a magnetic stirrer, flushed with nitrogen for 5 minutes and, when the bubbles in the solution disappeared, it was poured into a mold. The mold was made of two glass plates (13 cm × 13 cm) separated by a Teflon spacer, as shown in Figure 3.2. Spacers of two thicknesses were used : 1 58 mm and 2 38 mm.

TABLE 3.1. Gel Materials.

Material	Function	Mol. Wt.
N-isopropylacrylamide or NIPA $H_2C{=}CHCONHCH(CH_3)_2$	Monomer	113.18
N,N′- methylenebisacrylamide $(H_2C{=}CHCONH)_2CH_2$	Crosslinker	154.17
Sodium metabisulfite $Na_2S_2O_5$	Accelerator	190.10
Ammonium persulfate $(NH)_4S_2O_2$	Initiator	228.20

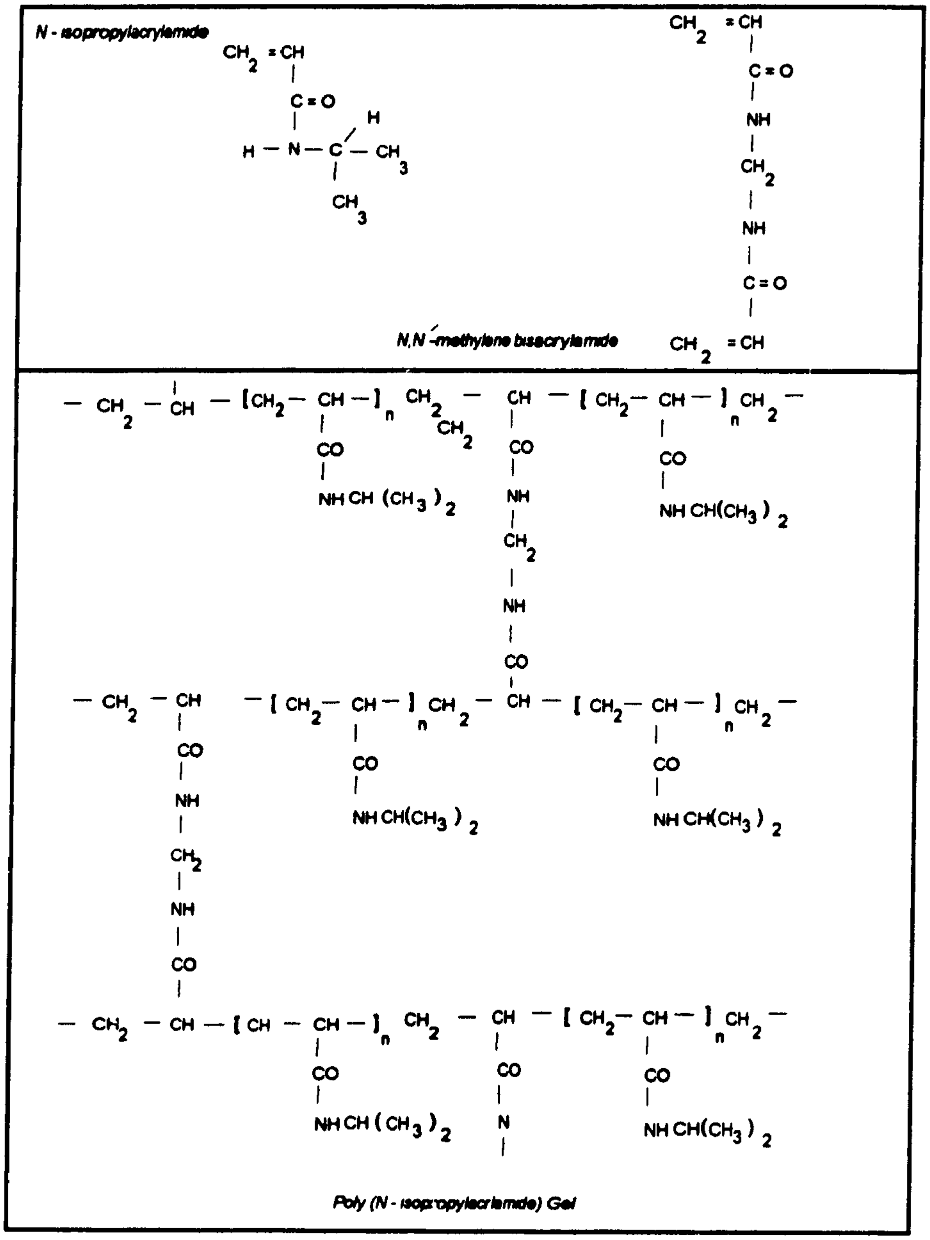

FIGURE 3.1. Molecular structure of the monomers and the poly(NIPA) gel.

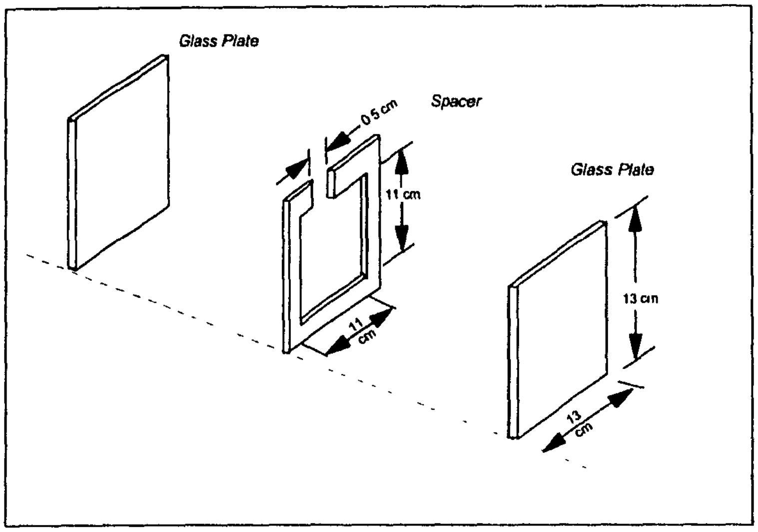

FIGURE 3.2. Glass plates and the spacer used for the gel mold

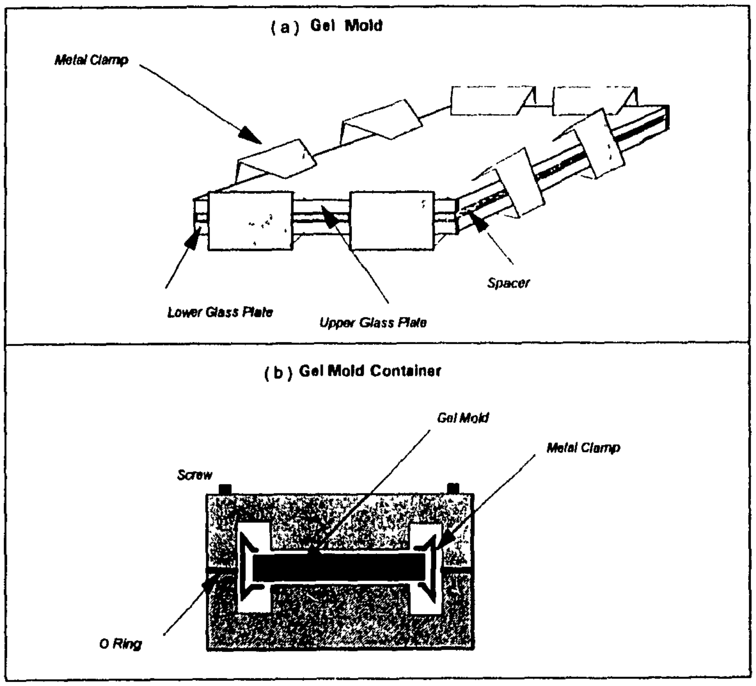

FIGURE 3.3. (a) Gel mold (for gelation at 15°C and 25°C) and the (b) aluminum gel mold container (for gelation at 15°C).

Polymerizations were carried out for 24 hours at 25°C or 15°C. For polymerization at 25°C, the mold containing the gel solution was pressed with metal clamps (see Figure 3.3.a) and the whole assembly was transferred to an airtight plastic container which was kept in a constant temperature room. For polymerization at 15°C, the gel mold was placed in a constant temperature water bath in an aluminum container (see Figure 3.3 b) to provide efficient heat transfer. After the polymerization was complete the gel sheet was removed from the mold and gel samples in the form of thin circular disks, 1 1 cm in diameter, were cut with a hollow cylindrical stainless steel cutter.

Table 3.2 shows the various gels synthesized at two different gelation temperatures. The ratio of the mass of accelerator and initiator added to the amount of total monomer was fixed at a value of one.

TABLE 3.2. Gel disks synthesized using different monomer concentration, percent crosslinker, gelation temperature and thickness.

Gel Characteristics	GELATION TEMPERATURE								
	T = 15° C					*T* = 25°C			
% T	15.6	15.6	15.6	10	10	10	10	10	10
% C	3.85	1.5	1.5	3.85	1.5	2.5	1.5	1.5	2.5
Thickness at Preparation (mm)	2.38	2.38	1.58	2.38	2.38	1.58	2.38	1.58	2.38

Following synthesis, the weight of gel disks at preparation, was measured to ± 0.0001 g with an electronic balance. Each gel piece was then dialyzed for 48 hours in deionized water at 23°C to remove unreacted monomers and oligomers trapped in the network. The water was replaced every 6-8 hours. The gels so obtained were then stored in 50 ml sealed glass bottles containing water at the room temperature.

Gel Collapse: The dialyzed gel pieces were separately immersed in deionized water contained in 250 ml bottles. To collapse the gels, these bottles were transferred to a constant temperature bath at 35°C. Following equilibration (3-5 days) the gels were ready for swelling experiments. The mass of the collapsed gel disks, *M*(c), was measured to ± 0 0001 g.

Gel Drying: Drying organic polymer gels is extremely difficult since they undergo considerable shrinkage and can warp or crack if the drying conditions are not carefully controlled. The gels were dried for 24 hours in a laboratory convective dryer maintained at 40°C. Only the equilibrated disks at 35°C could be dried without warping or cracking. The mass of the dry gel disks, *M*(d),was measured to ± 0.0001 g.

3.4. SWELLING EXPERIMENTS

3.4.1 PROCEDURE

The swelling experiments involved determination of transient weight changes of hydrogels at 25°C in 50 ml of unagitated water The approach to equilibrium was followed by periodically removing the suspended gel from the solution, blotting the excess water with a J-cloth, weighing it , and then returning it to the solution Equilibration times between 24 and 48 hours were used Most experiments were done with the collapsed gel samples equilibrated at 35°C, which is just above the poly(NIPA)-water phase-transition temperature of 34°C. These gels contained about 50 % water. A few experiments were carried with dried and preswollen gel samples

3.4.2 REPRODUCIBILITY

Gel disks, equilibrated at 35°C, were used as the starting materials for the swelling experiments performed at 25°C. Two tests were run. The first involved repeated swelling and collapse of a single gel sample The second involved a single swelling experiment on three disks cut from the same gel sheet.

Figure 3.4 shows the swelling data for a single gel disk plotted as the fractional approach to equilibrium, *F*, versus the square root of time in minutes. The $\sqrt{t}$ axis was chosen as the abscissa to display more information about the initial portions of swelling. Two swelling experiments are shown. At the start of Cycle 1 the disk was at 35°C, and then equilibrated at 25°C After equilibration, this disk was collapsed by raising the temperature of the gel-water system to 35°C . While the gel was collapsing, the solution was replaced every 6-8 hours. The equilibrated gel disk at 35°C marks the end of Cycle 1 and the beginning of Cycle 2, the second equilibration at 25°C The good repeatability demonstrates that

[a] The 48 hour dialysis removed the unreacted monomers, oligomers and other impurities.

[b] There was negligible loss of gel mass during the weighing procedure.

Figures 3 5 shows the swelling curves for three disks cut from the same sheet. The gel was made with 10 % T and 3.85 % C. Similar data are shown in Figure 3.6 for two disks cut from a gel sheet having 15 6 % T and 1.5 % C. The reproducibility of the swelling curves indicates that gelation was homogeneous throughout the sheet. Figure 3.7 shows swelling curves for two gel disks (15 % T, 3.85 % C) cut from sheets prepared separately under identical conditions. The reproducibility of the swelling curves for these replicates was very good.

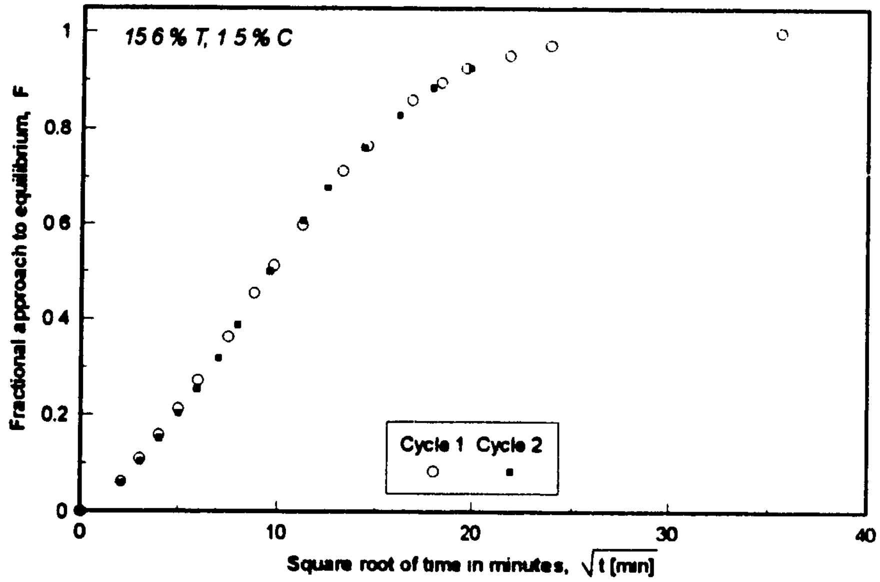

FIGURE 3.4. Two swelling cycles for same the gel specimen. Gelation and swelling temperatures were 15°C and 25°C, respectively. Initial dia. and thickness· 7.5 mm and 1.08 mm. [$\varphi_p^o = 0.59$ and $\varphi_p^{eq} = 0.0765$]

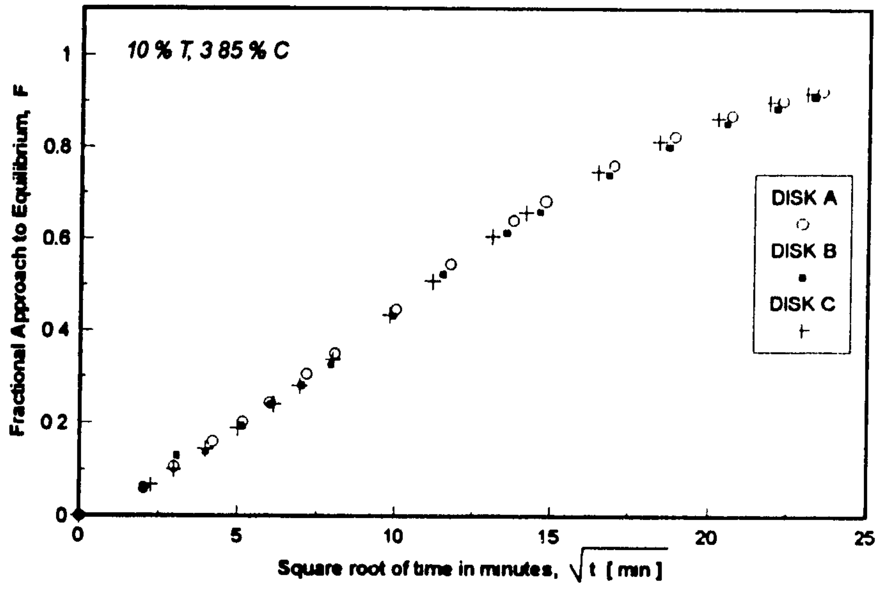

FIGURE 3.5. Swelling profiles for 3 poly[NIPA] disks (10% T and 3.85% C) cut from the same sheet. Gelation and swelling temperatures were 15°C and 25°C, respectively. Initial dia. and thickness: 7 mm and 1.28 mm.[$\varphi_p^o = 0.45$ and $\varphi_p^{eq} = 0.0844$]

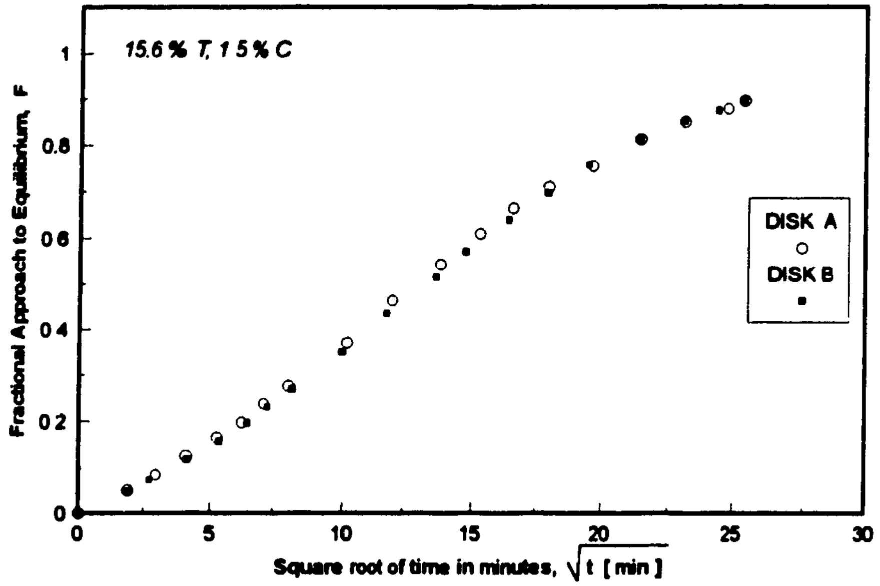

FIGURE 3.6. Swelling profiles for 2 poly(NIPA) disks (15.6% T and 1.5% C) cut from the same sheet. Gelation and swelling temperatures were 15°C and 25°C, respectively. Initial dia. and thickness: 6.95 mm and 1.46 mm. [$\varphi_p^o = 0.63$ and $\varphi_p^{eq} = 0.0774$]

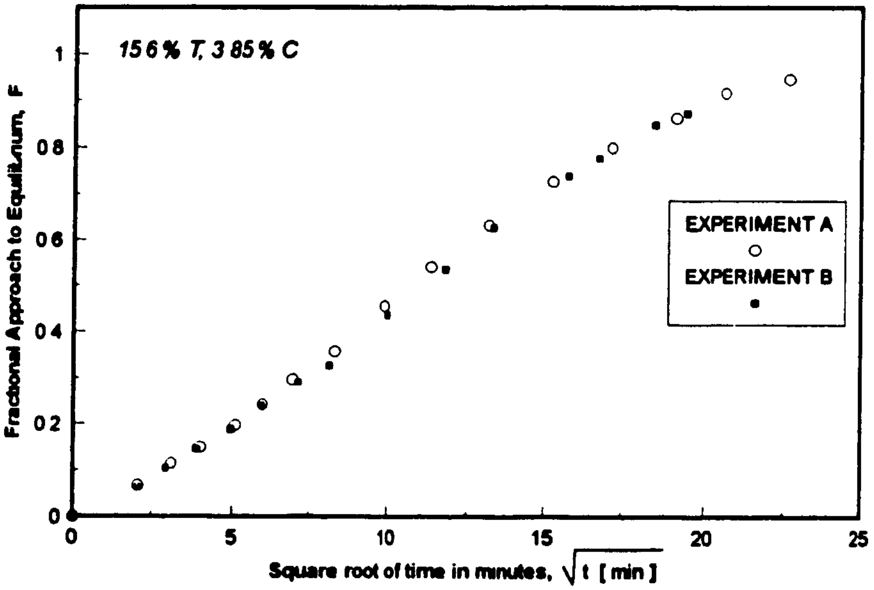

FIGURE 3.7. Replicate swelling profiles for 2 poly[NIPA] disks (15.6% T and 3.85% C) cut from different sheets. Gelation and swelling temperatures were 15°C and 25°C, respectively. Initial dia. and thickness: 7 mm and 1.4 mm. [$\varphi_p^o = 0.62$ and $\varphi_p^{eq} = 0.13$]

3.4.3 EFFECT OF GELATION TEMPERATURE

Figure 3 8 shows the swelling curves for disks with same thickness and composition: 10 % T and 1.5 % C, prepared at the two different temperatures The overlap of the swelling curves demonstrates that gelation temperature had only a small effect on the swelling kinetics.

The equilibrium mass ratios were expected to be different for the different gelation temperatures for the following reasons:

[a] Polymerization and crosslinking at lower temperature yields a slower reaction, which yields more crosslinks compared to a reaction at higher temperature

[b] At lower temperature the polymerizing chains are stretched out more (Treolar, 1975) than at higher temperature thus yielding a more homogeneous gel structure, i e there are fewer clusters of polymer chains (de-Gennes, 1979). Homogeneous gels swell slower compared to non homogeneous gels (Gehrke *et al.* 1991)

The implication of the above arguments is lower rates of swelling and lower equilibrium mass ratios for gels prepared at lower temperature The experimental data in Figure 3.8 show comparable swelling rates and equilibrium mass ratios for gelation at 25 °C and 15 °C, respectively

Poly(NIPA) gels with 15.6 % T and 3 85 % C were cloudy when gelation took place at 25°C, while gels with 10 %T and 1.5 %C were transparent After the first 5 minutes of polymerization at 15.6 % T and 3 85 % C , the forming polymer changed into a milky latex. Adjusting the % initiator and the % accelerator as suggested by Gehrke (1986), did not prevent cloudiness. However transparent gels were formed at 15.6 % T and 3.85 % C when the gelation temperature was 15°C The opaqueness of gels formed at 25 °C is probably due to slow dissipation of the heat of reaction so that the temperature inside the mold exceeds the polymer phase separation temperature (LCST at 32°C).

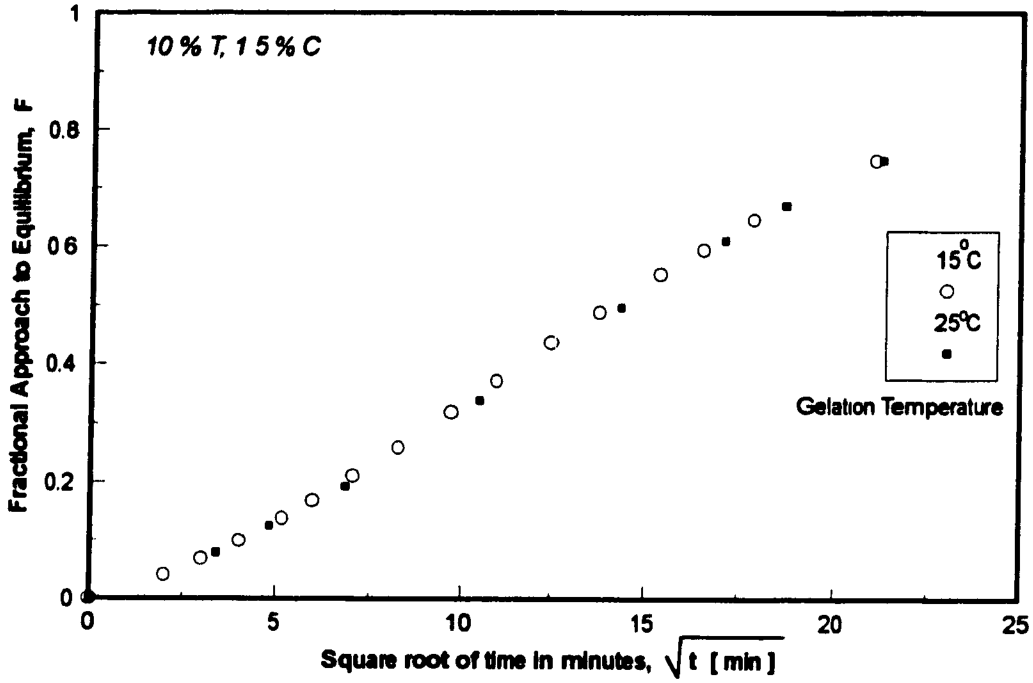

FIGURE 3.8. Effect of the gelation temperature on the swelling profiles of poly(NIPA) disks in water at 25 °C.

Gelation temperature	Initial thickness (mm)	Initial diameter (mm)	φ_p^o	φ_p^{eq}	Φ
15 °C	1.2	6 5	0.53	0.0433	12.2
25 °C	1.2	6.5	0.55	0.0458	12.0

3.4.4 EFFECT OF %T AND %C

The equilibrium mass ratio, Φ, for dry gel materials, is far higher, almost double, compared to that for collapsed gel materials. Table 3.3 compares Φ values for gels with different % T and % C.

TABLE 3.3. Comparison of equilibrium mass ratios for gels with different monomer concentration and percent crosslinker. The gelation and the swelling temperatures were 15°C and 25°C, respectively.

% T	% C	Φ	
		DRY	COLLAPSED
15.6	3.85	7.7	4.8
15.6	1.50	12.9	8.1
10.0	1.50	23.3	12.2
10.0	3.85	11.7	5 4

An increase in %T or %C leads to a lower equilibrium mass ratio. Increasing either %T or %C yields a gel network with more chain entanglements or crosslinks which limit gel expansion.

Figure 3 9 shows the swelling curves for four gels with different composition and crosslinker content synthesized at 15°C with the same thickness at preparation The disks had different diameters and thicknesses in the collapsed state at the start of swelling. All curves were sigmoidal. The curves with the same % C but different % T tend to be closer than curves with different % C Higher % T yields a lower equilibrium mass ratio, but faster equilibration.

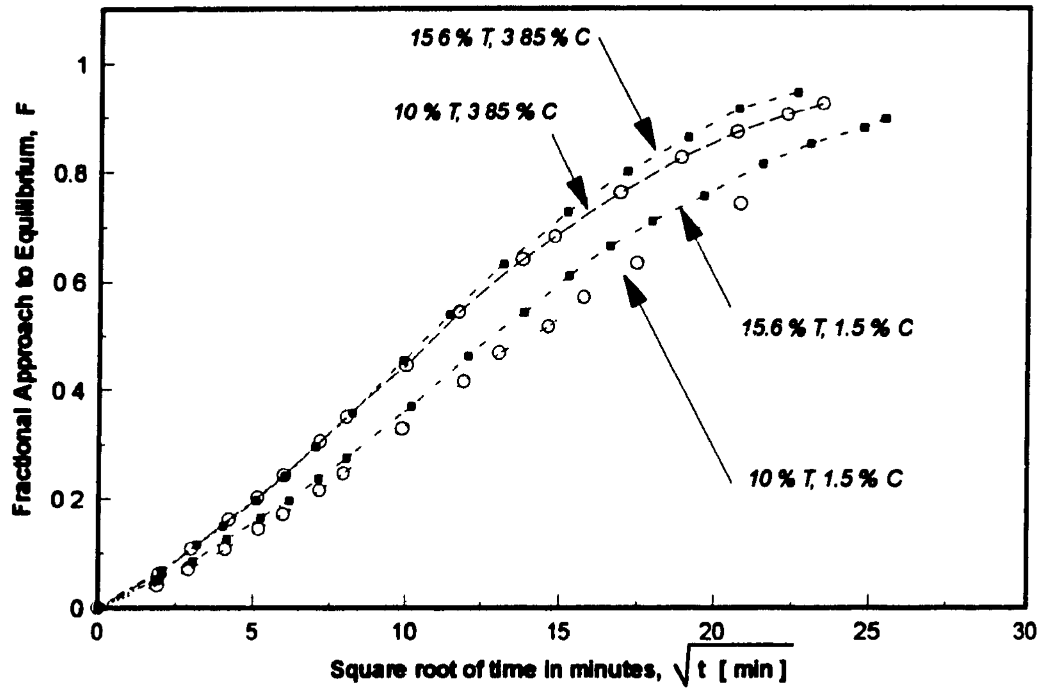

FIGURE 3.9. Effect of %T and %C on the swelling profiles of poly(NIPA) disks in water at 25 °C. The gelation temperature was 15°C

% T	% C	Initial thickness (mm)	Initial diameter (mm)	φ_p^o	φ_p^{eq}	Φ
15.6	3.85	1.40	7.00	0.62	0.13	4.8
10.0	3.85	1.28	7.00	0.45	0.0844	5.4
15.6	1.50	1.46	6.95	0.63	0.0774	8.1
10.0	1.50	1.20	6.50	0.53	0.0433	12.2

3.4.5 EFFECT OF THICKNESS

Figure 3.10 is a plot of F versus $\sqrt{(t)}/x_o$ for two gels having the same % T and % C but different thicknesses. Here x_o is the initial half thickness of the gel disk at time zero. Scaling the time axis brings the data for these thicknesses together

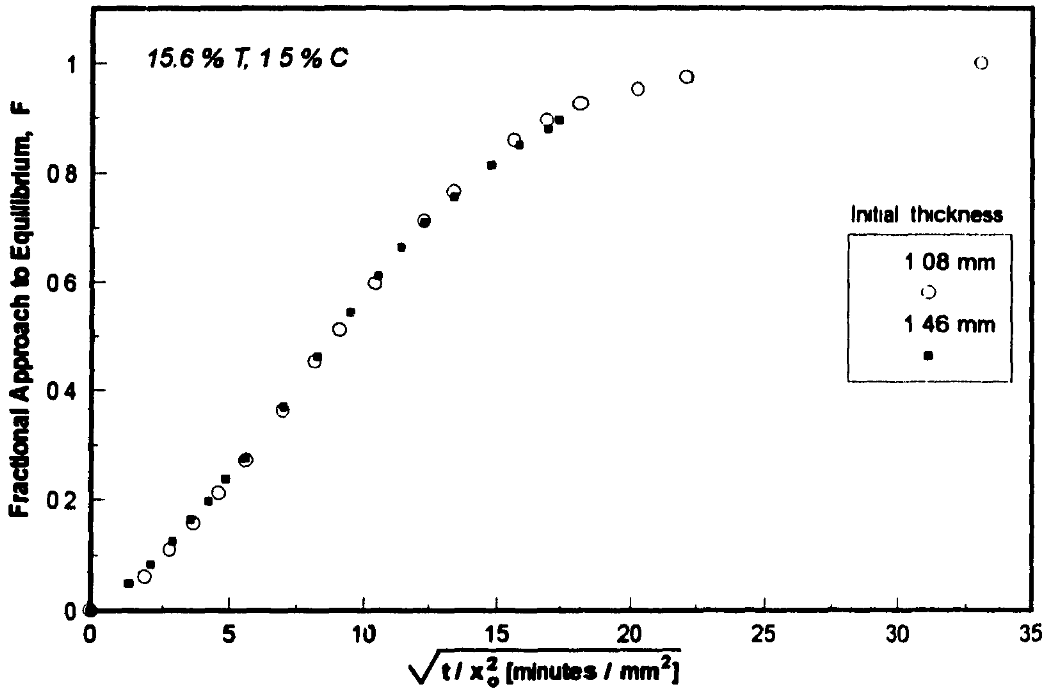

FIGURE 3.10. Effect of the initial thickness on the swelling profiles of poly(NIPA) disks in water at 25 °C.

Initial thickness (mm)	Initial diameter (mm)	Gelation temperature	φ_p^o	φ_p^{eq}	Φ
1.08	7.50	15 °C	0.59	0.0765	7.7
1.46	6.95	15 °C	0.63	0.0774	8.1

3.5. WHY IS THE SWELLING CURVE SIGMOIDAL ?

Figure 3.11 shows the swelling curves for collapsed and dry starting materials. It indicates sigmoidal swelling behavior.

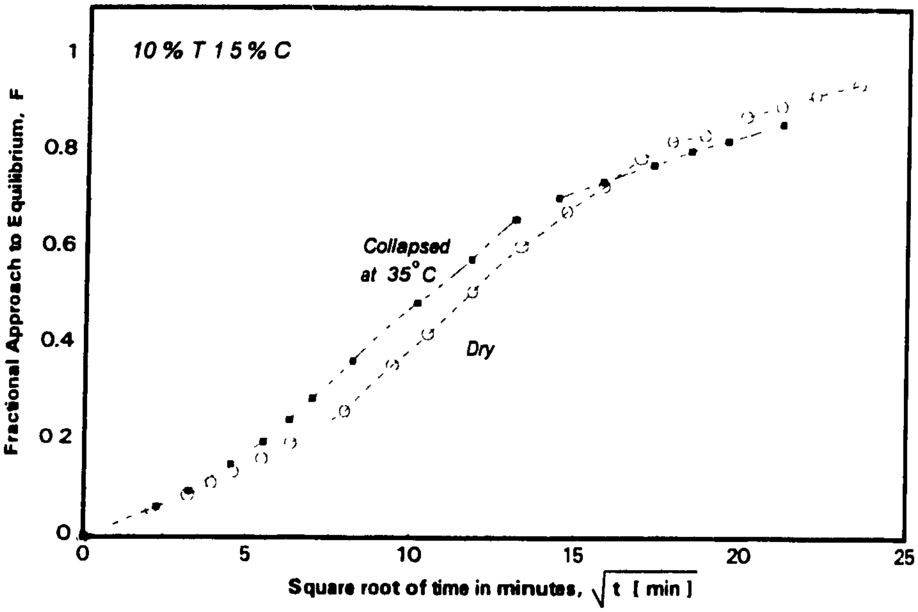

FIGURE 3.11. Effect of different starting points on the swelling profiles of poly(NIPA) disks in water. The gelation and the swelling temperatures were both equal to 25°C.
[$\varphi_p^{eq} = 0.043$, Collapsed: $\varphi_p^o = 0.5$, $\Phi = 11.6$, Dry $\varphi_p^o = 1$, $\Phi = 23.3$]

Following experimental observations may be responsible for the sigmoidal shape

[a] The range of swelling was too large.

[b] The disk geometry changed during swelling. After about five minutes of swelling, a collapsed disk *buckled.* It reacquires the disk shape about an hour later.

[c] The disk did not swell only in one direction; it swelled *isotropically.* This increased the gel surface area. Some evidence of isotropic swelling is given in Table 3.4.

TABLE 3.4 The mass, diameter, and thickness of various disks. The gelation and swelling temperatures were 15°C and 25°C, respectively.

% T	% C	Mass of the Gel (g)			Φ	Thickness (mm)			Diameter (mm)		
		M(d) Dry	M(c) Collapsed	M(∞) Swollen	M(∞)/M(c)	Collapsed	Swollen	Ratio	Collapsed	Swollen	Ratio
15.6	3.85	0.0304	0.0490	0.2341	4.8	1.40	2.28	1.63	7.0	11.5	1.64
15.6	1.50	0.0316	0.0500	0.4083	8.1	1.46	2.80	1.92	6.95	14.0	2.00
15.6	1.50	0.0226	0.0383	0.2954	7.7	1.08	1.94	1.80	7.5	14.0	1.87
10.0	3.85	0.0207	0.0459	0.2453	5.4	1.28	2.28	1.70	7.0	11.5	1.64
10.0	1.50	0.0209	0.0397	0.4824	12.2	1.20	2.70	2.25	6.5	14.5	2.23

In addition, several other phenomena were hypothesized to explain the sigmoidal shape of the swelling curves:

[1] The gel did not swell isothermally. The collapsed gel piece at 35°C was suddenly transferred into water at 25°C at time zero. The gel temperature decreased as it swelled.

[2] Anatomically the swollen and the collapsed gel pieces are different (See Figure 3.12). The left side of the schematic shows a nearly fully swollen gel piece at 25°C. Notice the macroscopic homogeneity in this case. The gel piece on the right side of the figure was collapsed at 35°C. The polymer chains, in the poly(NIPA) gel, form clusters above the phase transition temperature, leaving large patches of water in between (Gehrke, 1991). In light of these facts, it must take a finite time for the network to reorient itself topologically when a collapsed gel piece at 35°C is suddenly introduced into water at 25°C.

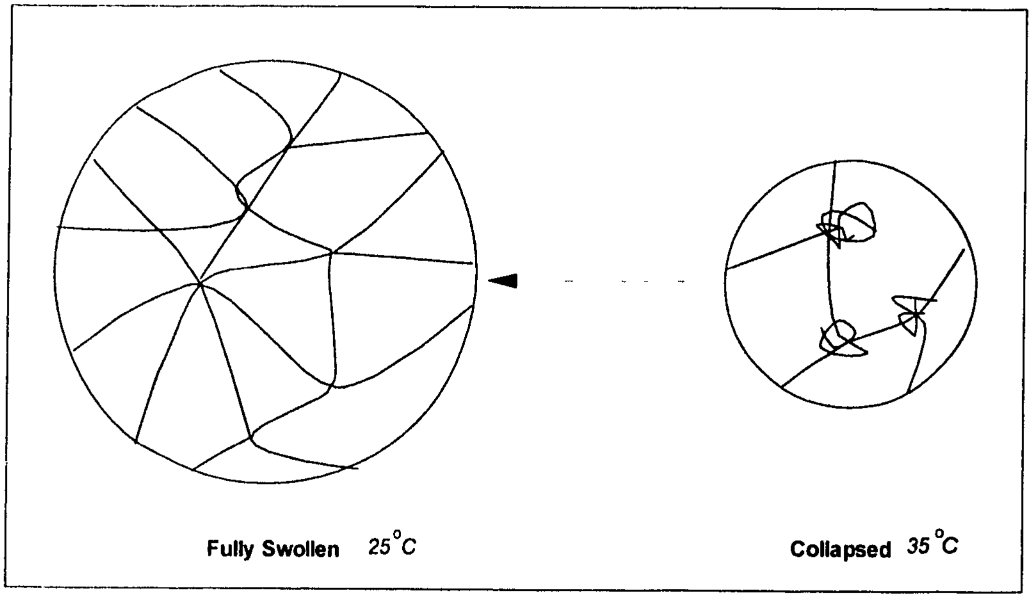

FIGURE 3.12. The swollen and the collapsed phases of the gel.

[3] The surface of a collapsed hydrogel is hydrophobic while the interior is hydrophilic (Peppas, 1986). For the first few minutes the diffusion of water into the gel is hindered as the polymer chains at the surface realign their hydrophilic and hydrophobic parts.

Experiments were performed to further investigate [b] and to test [1]. Figure 3.13 shows the swelling curves for three dry gel disks, each at a different temperature, at the onset of swelling. The swelling curves follow the same path for the initial 50 minutes All effects due to a different initial temperature of the disk apparently manifest during the later stages of swelling. An important question to be asked is, how long does the temperature gradient exist and how high is it? Simple calculations show that for a disk initially at 35°C, in equilibrium with water, when suddenly transferred into water at 25° C, it takes only 3 minutes for the temperature to fall to 26°C in the center.

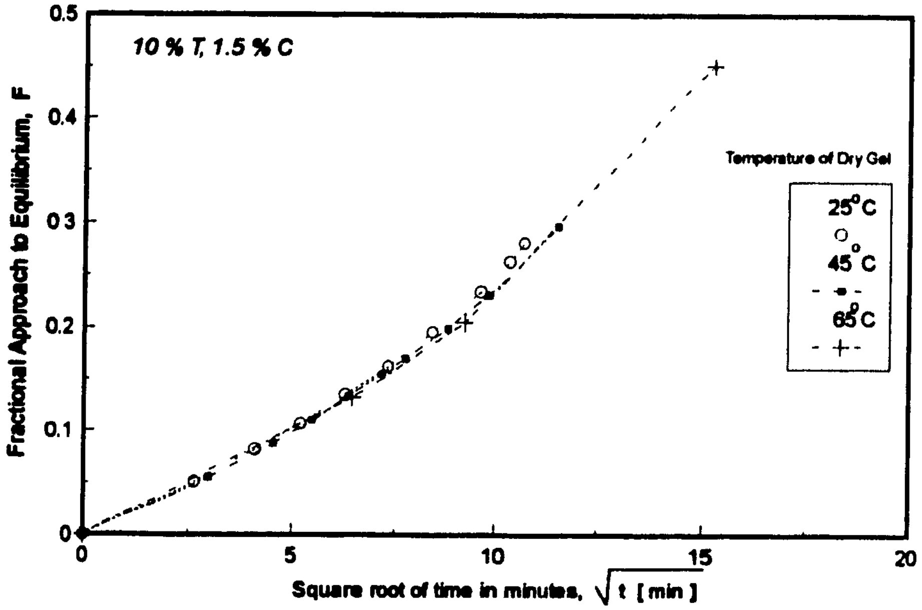

FIGURE 3.13. Effect of the initial temperature of a dry gel disk on the swelling profiles of poly(NIPA) disks in water. The gelation and swelling temperatures were both equal to 25°C. [$\varphi_p^o = 1$ and $\varphi_p^{eq} = 0.043$]

Another experiment was designed to investigate whether non-isothermal swelling was the real cause of the sigmoidal shape of the swelling curve. A collapsed disk at 35 °C, was removed from water and then transferred rapidly into a closed vessel containing water-saturated air at 25°C. After about 5 minutes, the disk now at approximately 25°C, was transferred into water at 25°C for swelling. The swelling curve was again indicated sigmoidal as shown in Figure 3.14.

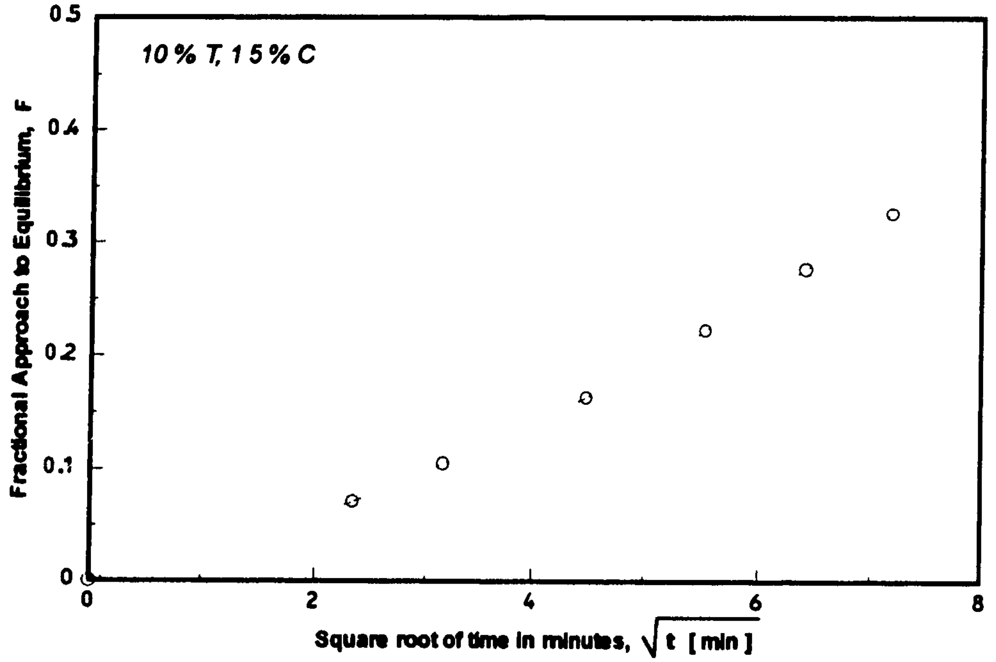

FIGURE 3.14. Poly(NIPA) disk at 25 °C at the start of the swelling experiment. The gelation and the swelling temperatures were both equal to 25°C. [$\varphi_p^o = 0.5$ and $\varphi_p^{eq} = 0.043$]

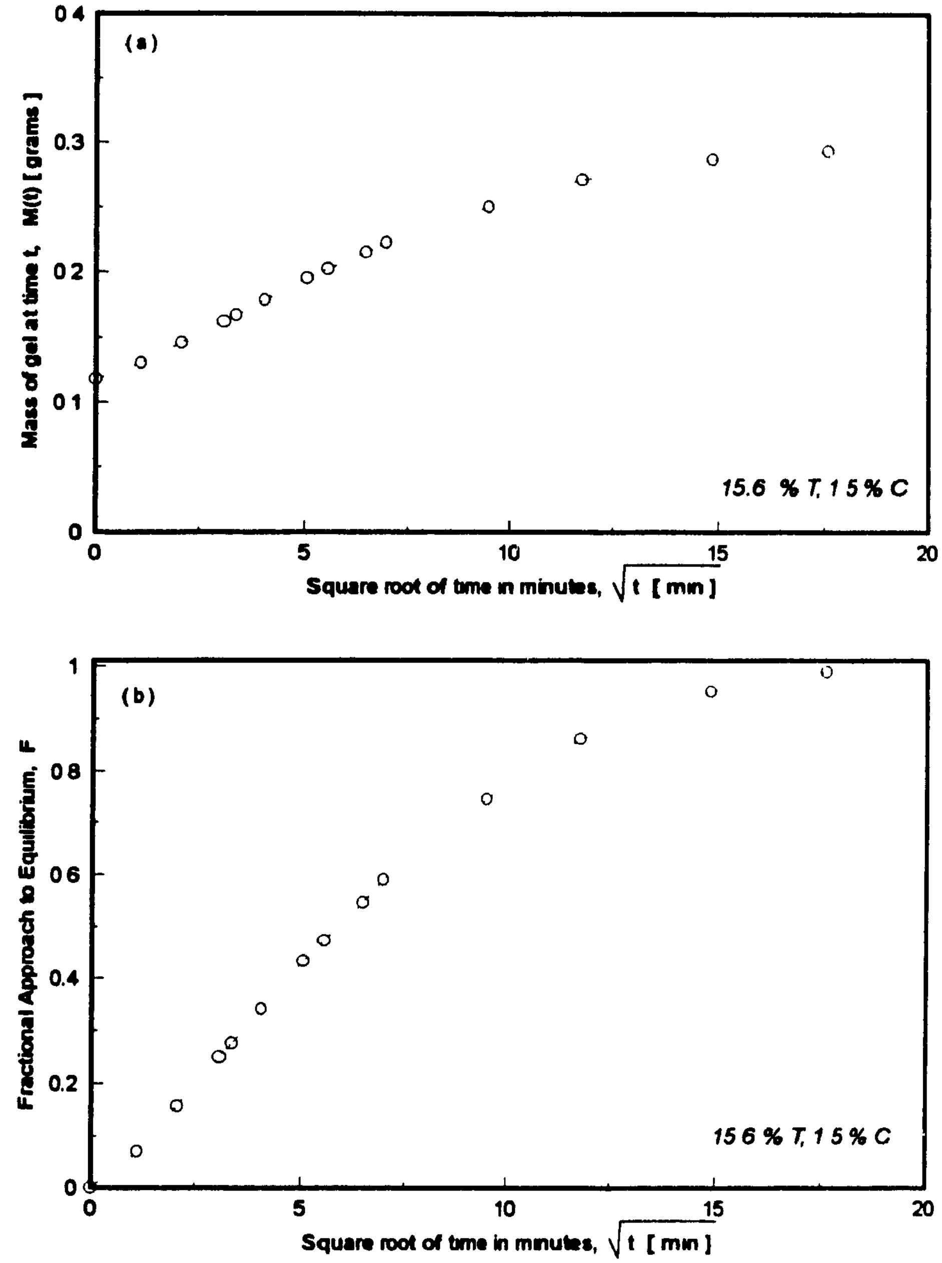

FIGURE 3.15 Swelling curve for starting point close to equilibrium on (a) $M(t)$ versus $\sqrt{t}$. and on (b) F versus $\sqrt{t}$. The gelation temperature and the swelling temperature were 15°C and 25°C, respectively.

Initial diameter (mm)	Initial thickness (mm)	φ_p^o	φ_p^{eq}	Φ
10	1	0.19	0.0765	2.5

In another experiment, poly(NIPA) gel disks, prepared as described in section 3.3, were placed into cylindrical cavities (10 mm dia.), produced by clamping between glass plates 1 mm thick Teflon sheet through which circular holes were punched. A collapsed disk was placed in each hole and the remaining volume filled with water. The assembly was pressed tightly with metal clamps and left in the horizontal position until the gel disks attained the size of the cavities by sorption of the water. The disks prepared in this way contained approximately 80 % water. After equilibration at 25°C for 12 hours the disks were removed and swollen in water at 25°C. The gel was isothermal throughout the course of swelling.

Figures 3.15a and 3.15b show the swelling curves for one of these disks plotted as mass and fractional approach to equilibrium versus square root of time. The curves were sigmoidal, but the sigmoid was less pronounced than for swelling of a collapsed gel. For the preswollen gel in Figure 3.15b, $\Phi = 2.5$, while for the collapsed gel in Figure 3.6, $\Phi = 7.7$. The preswollen gel did not buckle during swelling, thus demonstrating that sigmoidal shape of the swelling curve is not due to buckling.

The experimental evidence shows that the sigmoidal swelling behavior of poly(NIPA) gel disks is not caused by non-isothermal conditions nor the change of shape due to buckling. The most likely reason is the large range of swelling.

CHAPTER 4

Comparison of Model with Experiments

4.1. INTRODUCTION

The moving boundary model for the kinetics of gel volume change with a constant D_m was solved numerically for the three one-dimensional geometries slabs, cylinders and spheres. The results are presented in dimensionless form The model with a constant and a variable D_m is then compared with the experimental results for the swelling of poly(NIPA) disks in water Comparisons are also made with the data of Tanaka *et al.* for the swelling of polyacrylamide beads (1979) and the collapse of poly(NIPA) beads (1985) in water Finally, comparisons are made with the data obtained by Mazich *et al.* (1992) for the swelling of polyisoprene spheres in toluene Various theoretical and empirical forms of the composition-dependent diffusion coefficient were used to fit the experimental data

4.2. METHOD OF SOLUTION

4.2.1 NUMERICAL COMPUTATION OF MOVING BOUNDARY PROBLEM

Coupled gel diffusion and interface motion is solved numerically in a system of coordinates where the position of the boundary remains fixed The dimensionless coordinate r^* is defined by

$$r^* = \frac{r}{R(t)} \qquad [4.1]$$

where $R(t)$ is the position of the boundary at time t; hence the governing equations are solved within the fixed domain $0 \le r^* \le 1$ The dimensionless time, τ_o, is defined by

$$\tau_o = \frac{t\, D_m}{R_o^2} \qquad [4.2]$$

where R_o is the initial position of the boundary: half thickness of a disk, the radius of a cylinder or the radius of a sphere. The dimensionless polymer volume fraction, φ^* is

$$\varphi^* = \frac{\varphi_p^\circ - \varphi_p}{\Delta \varphi_p} \qquad [4.3]$$

where

$$\Delta \varphi_p = \varphi_p^\circ - \varphi_p^{eq} \qquad [4.4]$$

and φ_p^o and φ_p^{eq} are the initial and final polymer volume fractions in the gel, respectively Appendix III contains a derivation of the gel volume change equations in terms of r^*, τ_o and φ^* for constant D_m The final equations are as follows

GEL DIFFUSION EQUATION:

$$\frac{\partial \varphi^*}{\partial \tau_o} = \frac{r^*}{r^\circ} \frac{\partial \varphi^*}{\partial r^*} \frac{\partial r^\circ}{\partial \tau_o} + \left(\frac{1}{r^\circ}\right)^2 \left[\frac{i}{r^*} \left(\frac{\partial \varphi^*}{\partial r^*} \right) + \frac{\partial^2 \varphi^*}{\partial r^{*2}} \right] \qquad [4.5]$$

where

$$r^\circ = \frac{R(t)}{R_o} \qquad [4.6]$$

and $i = 0$, 1 and 2 for a slab, a cylinder and a sphere, respectively.

INTERFACE EQUATION:

$$\frac{dr^{\circ}}{d\tau_{\circ}} = [\Phi - 1]\frac{1}{r^{\circ}}\left.\frac{\partial \varphi^{*}}{\partial r^{*}}\right|_{r^{*}=1} \qquad [4.7]$$

where

$$\Phi = \frac{\varphi_p^{\circ}}{\varphi_p^{eq}} \qquad [4\ 8]$$

The boundary and initial conditions for Equation 4.5 are

$$\text{at } \tau_{\circ} = 0 \qquad \varphi^{*} = 0 \qquad \text{for} \qquad 0 \le r^{*} \le 1 \qquad [4\ 9a]$$

$$\text{at } r^{*} = 1 \qquad \varphi^{*} = 1 \qquad \text{for} \qquad \tau_{\circ} > 0 \qquad [4\ 9b]$$

$$\text{at } r^{*} = 0 \qquad \frac{\partial \varphi^{*}}{\partial r^{*}} = 0 \qquad \text{for} \qquad \tau_{\circ} \ge 0 \qquad [4\ 9c]$$

The initial condition for Equation 4.7 is

$$\text{at } \tau_{\circ} = 0 \qquad r^{\circ} = 1 \qquad [4.10]$$

Equations 4.5 to 4.10 apply for swelling ($\varphi_p^o > \varphi_p^{eq}$) and collapse ($\varphi_p^o < \varphi_p^{eq}$). The only parameter in these dimensionless equations is Φ, as given by Equation 4 8 Φ can also be expressed as

$$\Phi = \frac{V(\infty)}{V(0)} \qquad [3\ 3b]$$

where $V(\infty)$ and $V(0)$ are the volumes of the gel at equilibrium and at the start of swelling (or collapse), respectively For constant and equal polymer and solvent densities, equilibrium volume ratio is the same as the equilibrium mass ratio

The finite difference method of Sparrow and Chuck (1984) was used to solve Equations 4.5 to 4.10. An implicit scheme was used for the gel-diffusion equation and an explicit scheme for the interface equation. The discretization, and the convergence and accuracy of the numerical computations are discussed in Appendices III and IV.

For a composition dependent diffusion coefficient, Equation 4.5 becomes

$$\left[\frac{\partial \varphi^*}{\partial t}-\frac{r^*}{r^\circ}\frac{\partial \varphi^*}{\partial r^*}\frac{d r^\circ}{d t}\right]=\left(\frac{1}{r^\circ R_\circ}\right)^2\left[\frac{i D_m}{r^*}\left(\frac{\partial \varphi^*}{\partial r^*}\right)+D_m\frac{\partial^2 \varphi^*}{\partial r^{*2}}+\frac{\partial D_m}{\partial \varphi^*}\left(\frac{\partial \varphi^*}{\partial r^*}\right)^2\right] \quad [4\ 11]$$

This equation was solved in the dimensional form using the same numerical technique

4.2.2. FRACTIONAL APPROACH TO EQUILIBRIUM

The fractional approach to equilibrium, F, was computed from the profiles of φ^* versus r^* by

$$F=\left(\frac{\Phi/\hat{\Phi}-1}{\Phi-1}\right) \quad [4.12]$$

where $\hat{\Phi}$ is the ratio of the instantaneous volumetric-average polymer volume fraction, $\hat{\varphi}_p$, and the equilibrium polymer volume fraction, φ_p^{eq}:

$$\hat{\Phi}=\frac{\hat{\varphi}_p}{\varphi_p^{eq}}=(i+1)\left(r^\circ\right)^{i+1}\int_0^1\left[\Phi-\{\Phi-1\}\,\varphi^*(r^*,\tau_\circ)\right]dr^* \quad [4\ 13]$$

where i = 0, 1, 2, for slabs, cylinders and spheres, respectively. The variable F runs from zero to one in both swelling and collapse.

4.3. ONE DIMENSIONAL VOLUME CHANGE WITH CONSTANT D_m

Figures 4.1, 4.2 and 4.3 show the swelling curves with constant D_m for slabs, cylinders and spheres, respectively. The fractional approach to equilibrium, F, is plotted against the square root of dimensionless time, $\sqrt{\tau_o}$

The shape of the swelling curves is contingent on the ratio of the final to initial polymer volume fraction, Φ, in addition to the the sample geometry For a given Φ value, regardless of the geometry, the plot of F vs $\sqrt{\tau_o}$ yields a single curve The curve with a Φ value of 2, is the solution for all following different initial and final polymer volume fractions: 1 and 0.5; 0 8 and 0 4; 0.6 and 0 3, 0 2 and 0 1, etc The curve for $\Phi \rightarrow 1$ is for sorption without volume change. For this case, called Fickian II in Chapter 2, the sorption is described by Fick's second law without boundary motion Appendix IV shows the results of the numerical computations for Φ near one

The swelling curves for slabs appear different from those for cylinders and spheres For slabs the swelling curves are initially linear For cylinders and spheres, curves with Φ values above about 2 are sigmoidal. A point of inflection occurs where a change in the sign of the second derivative of F with respect to $\sqrt{\tau_o}$ takes place If the swelling curve is sigmoidal, the second derivative is positive initially, decreases to zero at the point of inflection, and then becomes negative The numerical values of the second derivative, computed by the three point central difference formula, are shown in Figure 4 4 as a function of $\sqrt{\tau_o}$ for a sphere Computations were made for various Φ values No inflection point was found for swelling curve with $\Phi = 2$ For curves with $\Phi > 2$, the infection point appears For the same value of Φ, the inflection point for a cylinder occurs at a smaller value of F than for a sphere No inflection points were found for slabs even for a Φ value as high as 100 The increase in surface area for cylinders and spheres is probably responsible for the sigmoidal shape at $\Phi > 2$.

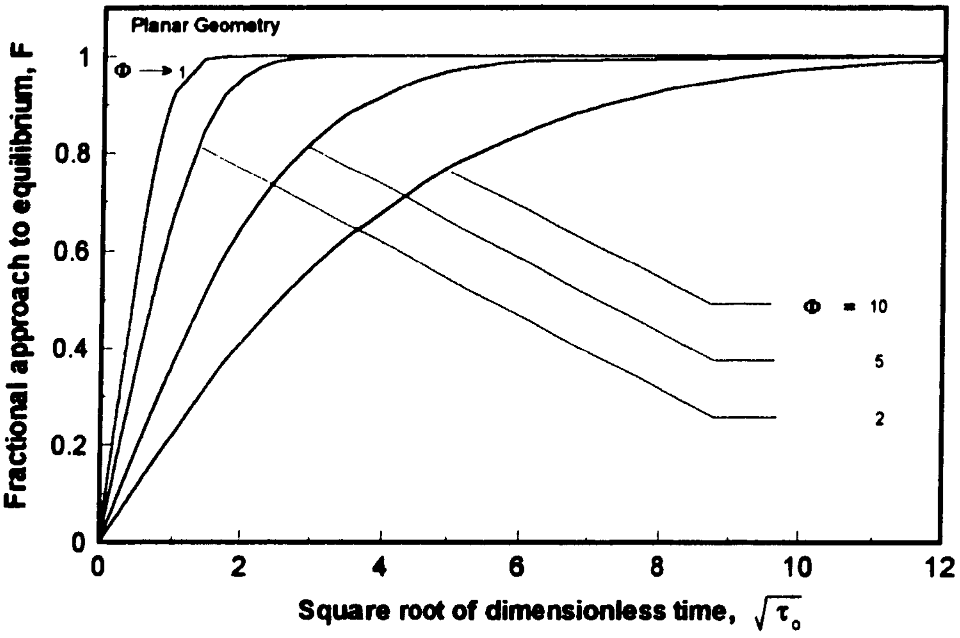

FIGURE 4.1. Swelling curves for slabs with constant D_m for different values of Φ.

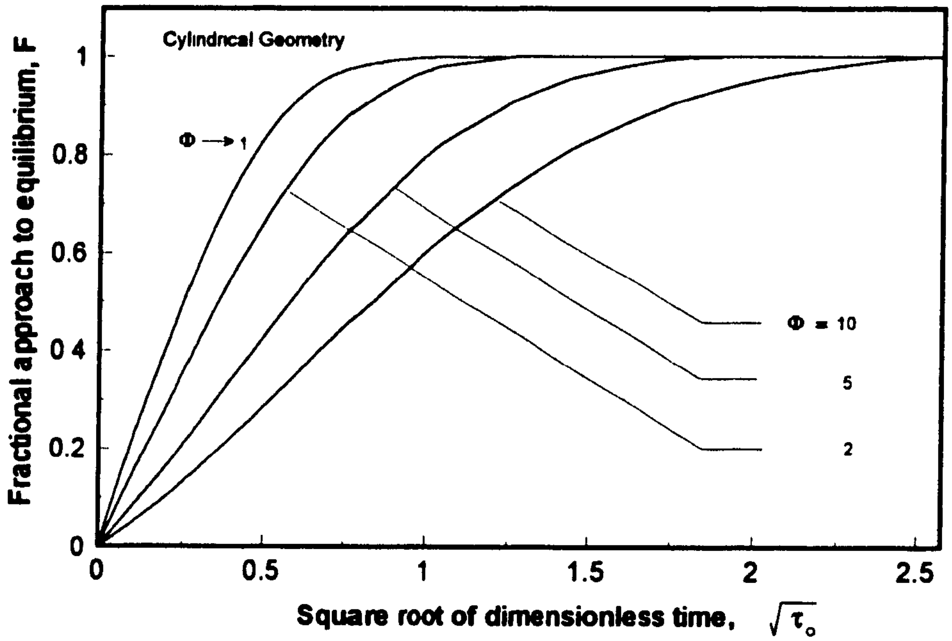

FIGURE 4.2. Swelling curves for cylinders with constant D_m for different values of Φ.

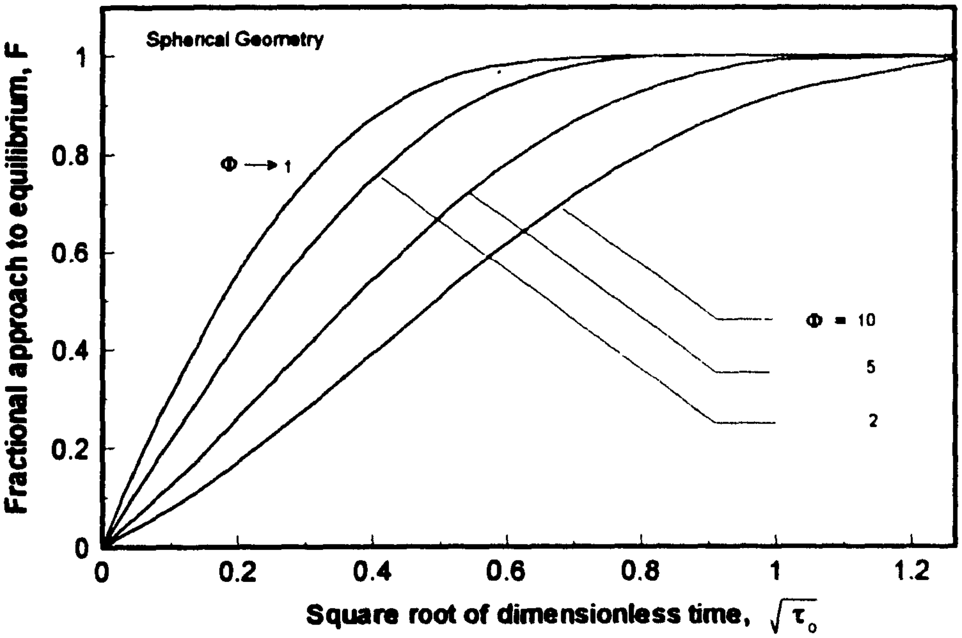

FIGURE 4.3. Swelling curves for spheres with constant D_m for different values of Φ.

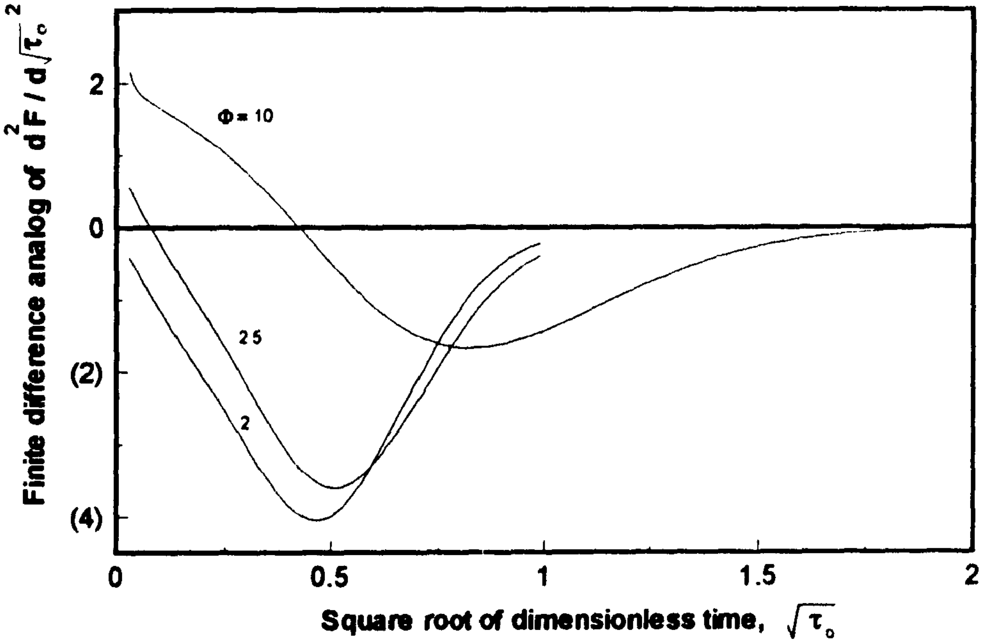

FIGURE 4.4. Finite difference analog of the second derivative of F with respect to τ_0 for spherical swelling curves. The numbers on the curves are the different values of Φ.

The swelling and collapse (sorption and desorption) curves for the three geometries are presented in Figures 4.5 and 4.6. To compare between the rates of swelling and collapse more easily, the dimensionless time used in these figures was

$$\tau_p = \frac{t\,D_m}{R_p^2} \qquad [4\ 14]$$

where R_p is the radius of the equivalent polymer sphere or a cylinder; or the half thickness of equivalent polymer disk, i.e. the characteristic dimension of the solvent free gel. The polymer equivalent radius is related to the initial radius at the start of swelling or collapse by

$$R_p = \left[\varphi^{\frac{1}{i+1}}\right] R_o \qquad [4.15]$$

i = 0, 1 and 2 for a slab, a cylinder and a sphere, respectively For a given gel piece, the quantity R_p is fixed , whereas R_o is larger for collapse than it is for swelling.

Figures 4.5 and 4 6, reveal that spheres swell and collapse the fastest and slabs the slowest. Collapse is faster than swelling for spheres, approximately the same as swelling for cylinders, and slower than swelling for slabs The swelling and collapse curves for spheres and cylinders cross; the curves for slabs do not This difference is attributed to the change in surface area which occurs for spheres and cylinders as swelling and collapse occur. There is no surface area change for a slab

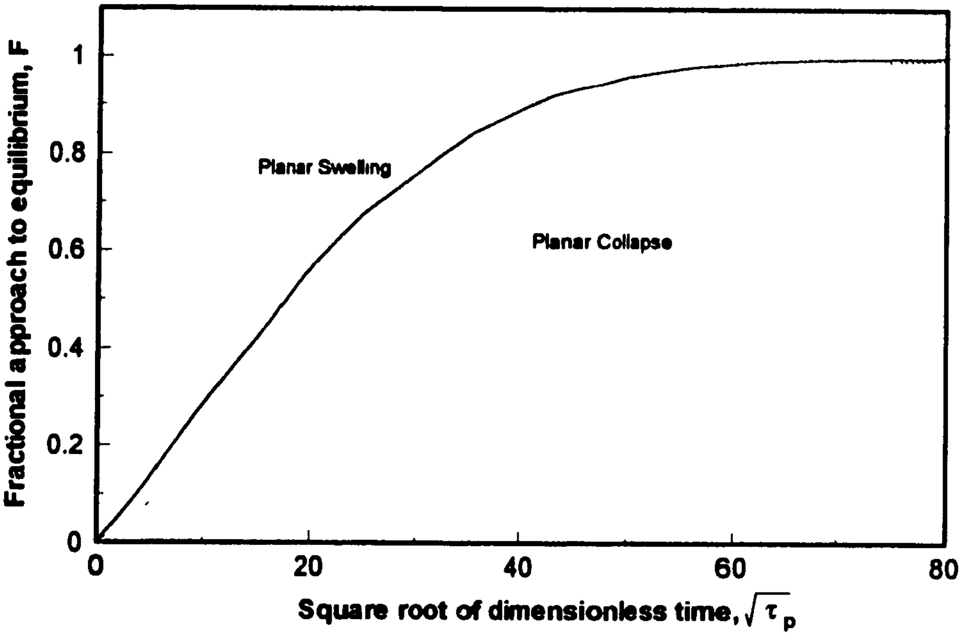

FIGURE 4.5. Comparison of swelling and collapse for planar geometry.
[Swelling: $\varphi_p^o = 0.2$, $\varphi_p^{eq} = 0.1$, $\Phi = 2$; Collapse: $\varphi_p^o = 0.1$, $\varphi_p^{eq} = 0.2$, $\Phi = 0.5$]

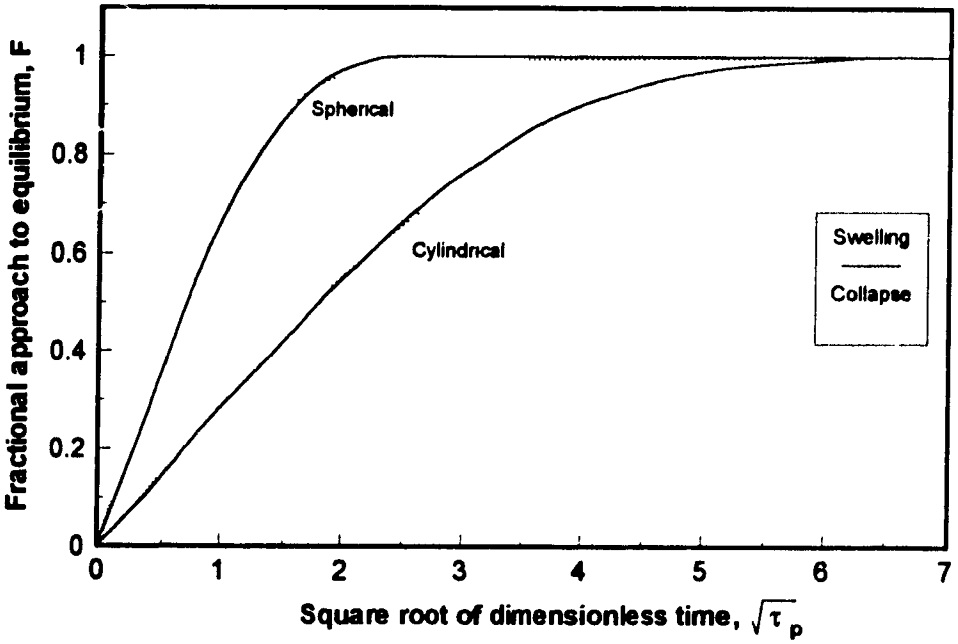

FIGURE 4.6. Comparison of swelling and collapse for spherical and cylindrical geometries.
[Swelling: $\varphi_p^o = 0.2$, $\varphi_p^{eq} = 0.1$, $\Phi = 2$; Collapse: $\varphi_p^o = 0.1$, $\varphi_p^{eq} = 0.2$, $\Phi = 0.5$]

Figures 4.7, 4.8 and 4.9 show the concentration profiles for several dimensionless times, τ_p, for spheres, cylinders and slabs, respectively. The volume fraction is plotted against r^o, where from Equations 4.6 and 4.14:

$$r^{\circ} = 1 \qquad \text{at} \quad \tau_p = 0 \qquad [4.16]$$

For swelling, r^o increases from 1 and for collapse r^o decreases from 1. At short times, the curves show sharp gradients near the moving boundary.

4.4 ESTIMATION OF THE DIFFUSION COEFFICIENT

The only unknown in the model is the diffusion coefficient, D_m. Several equations were proposed for D_m and the parameter(s) were estimated by minimizing the following objective function:

$$\Re = \sum_{i=1}^{n} \left[F_i^{\exp} - F_i^{\text{model}} \right]^2 \qquad [4.17]$$

where n is the number of experimental points.

A PASCAL program OPTIM, which uses Powell's method of conjugate directions (Press et al., 1989), was used to obtain the unconstrained minimum of the objective function.

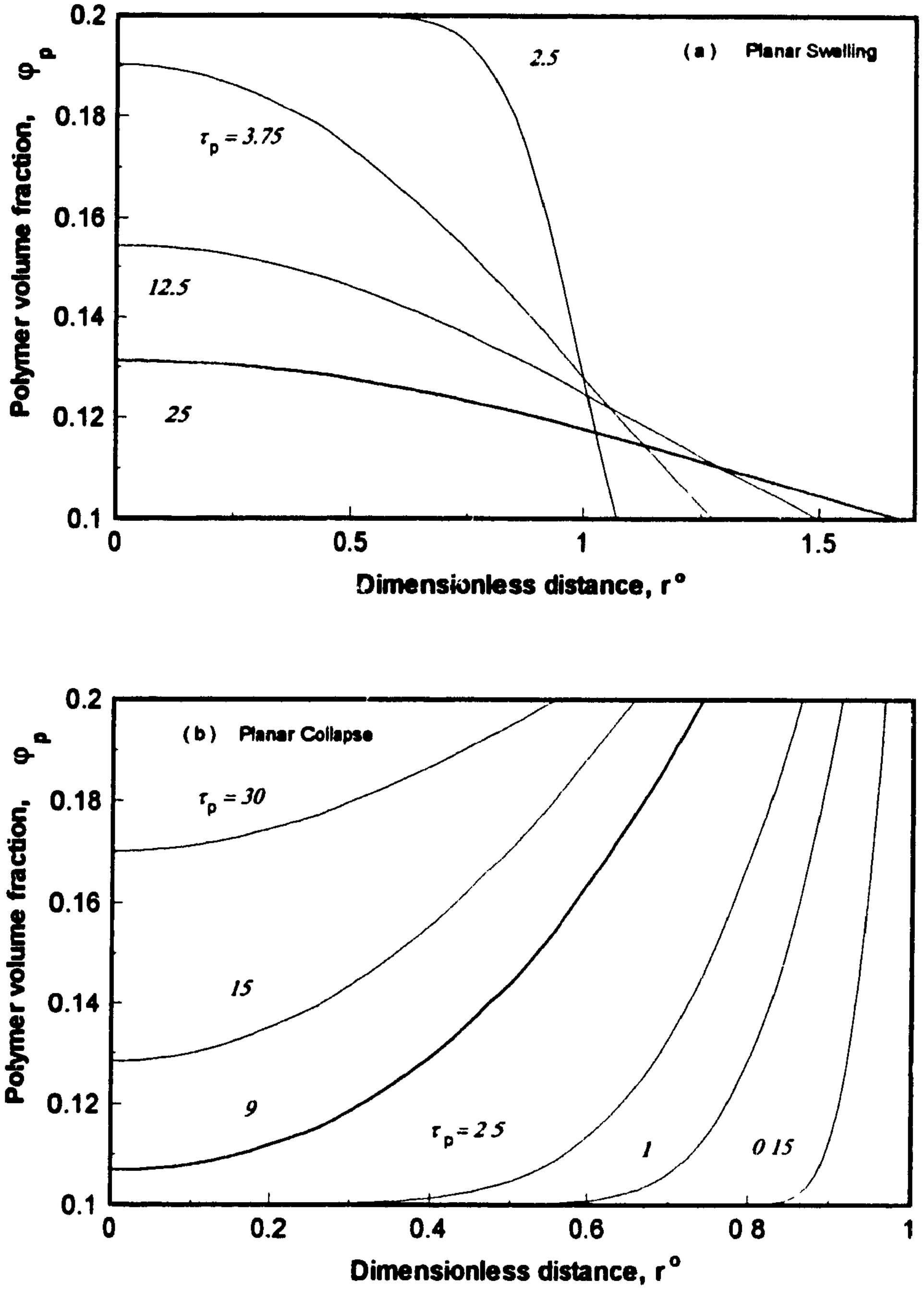

FIGURE 4.7. Concentration profiles for slabs at various dimensionless times, τ_p
(a) Swelling: $\varphi_p^o = 0.2$, $\varphi_p^{eq} = 0.1$, $\Phi = 2$ (b) Collapse: $\varphi_p^o = 0.1$, $\varphi_p^{eq} = 0.2$, $\Phi = 0.5$.

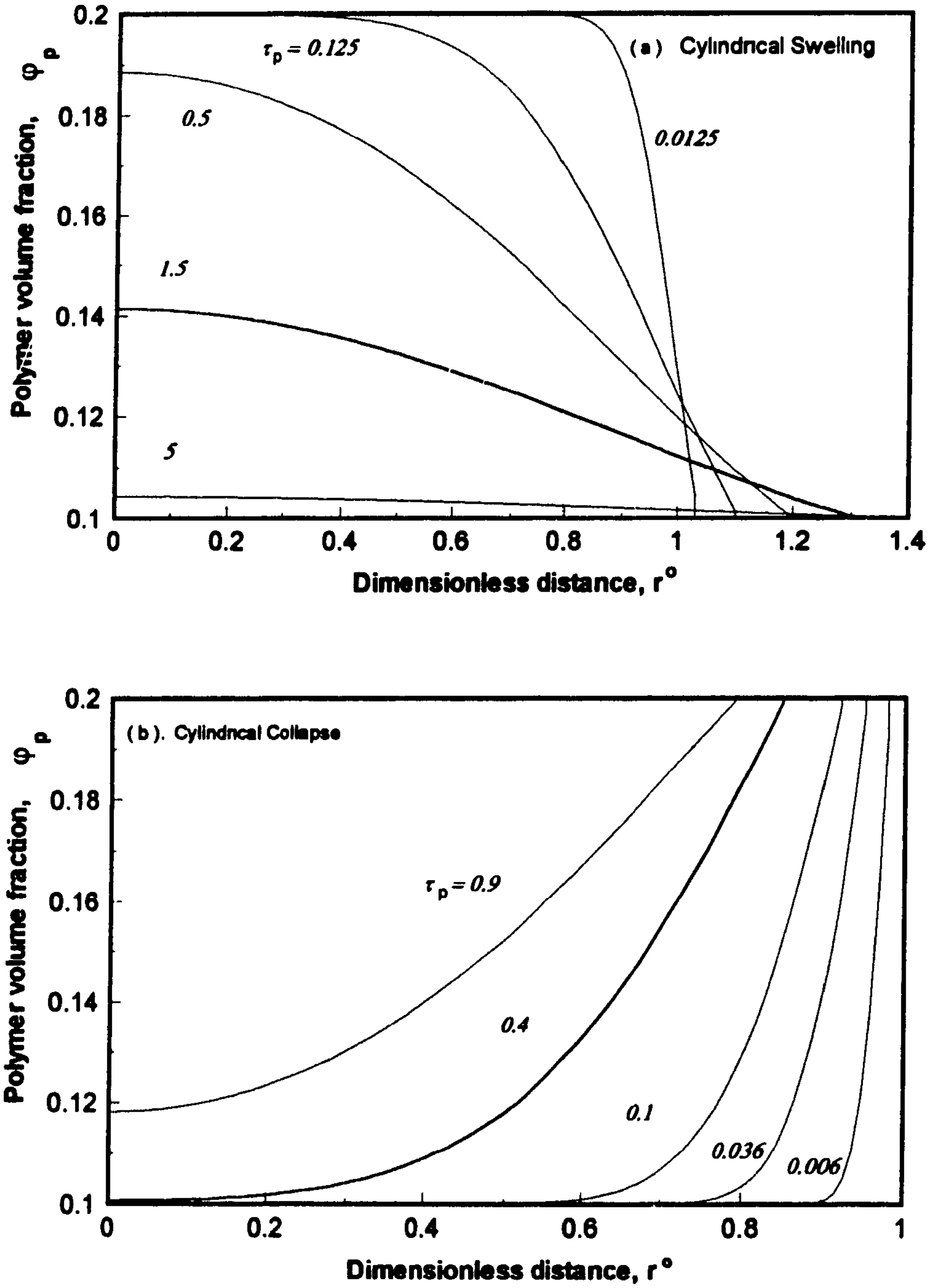

FIGURE 4.8. Concentration profiles for cylinders at various dimensionless times, τ_p
(a) Swelling: $\varphi_p^o = 0.2$, $\varphi_p^{eq} = 0.1$, $\Phi = 2$ (b) Collapse: $\varphi_p^o = 0.1$, $\varphi_p^{eq} = 0.2$, $\Phi = 0.5$.

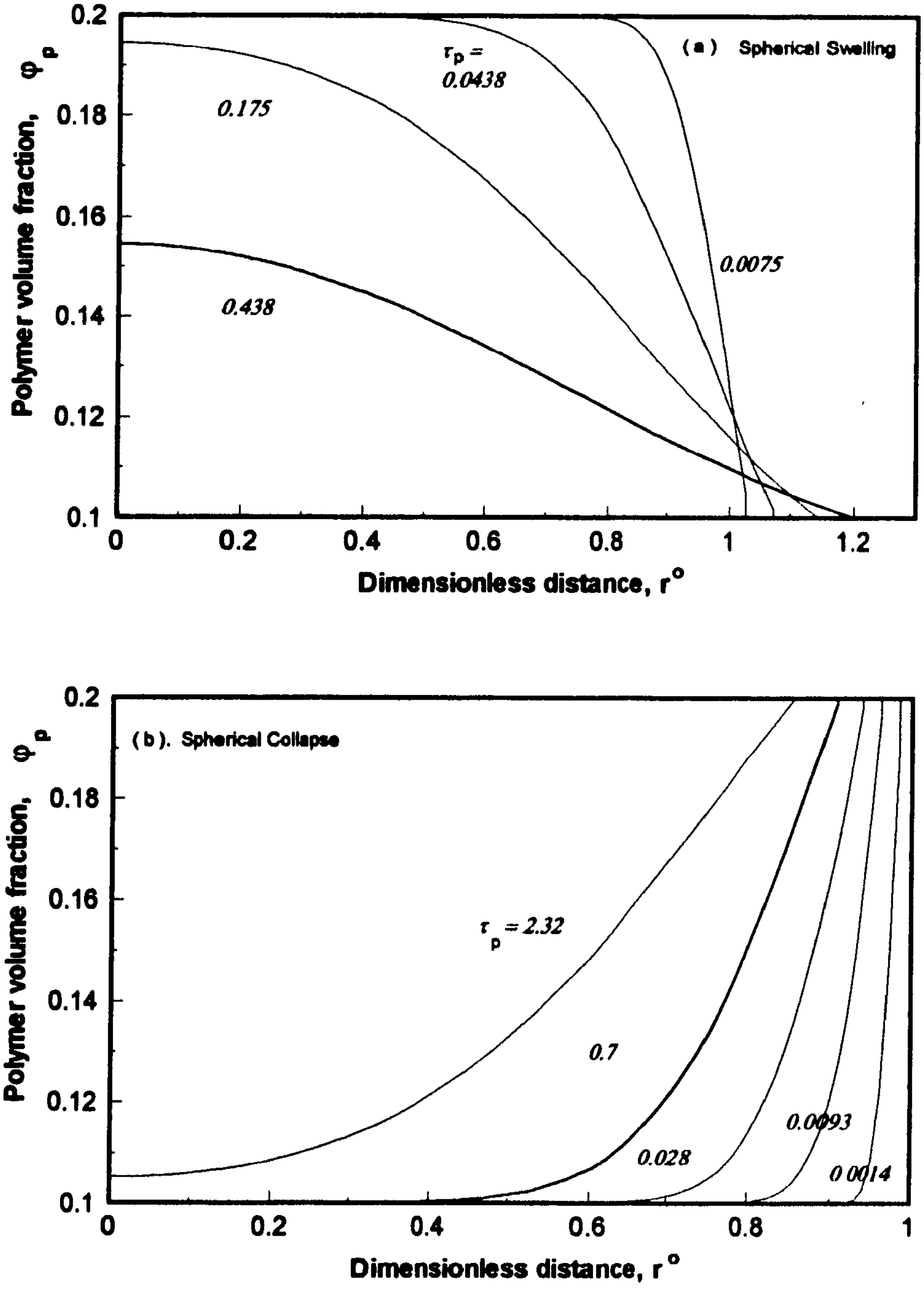

FIGURE 4.9. Concentration profiles for spheres at various dimensionless times, τ_p (a) Swelling: $\varphi_p^o = 0.2$, $\varphi_p^{eq} = 0.1$, $\Phi = 2$ (b) Collapse: $\varphi_p^o = 0.1$, $\varphi_p^{eq} = 0.2$, $\Phi = 0.5$.

4.5. FITTING THE MODEL TO DATA FOR *POLY [NIPA]* GEL DISKS

The ratios of the equilibrium to initial diameters and thicknesses were essentially equal (See Table 3 4). Therefore, one dimensional planar geometry does not represent the disks used in the experiments. Since the volume change was isotropic and the lateral surface of the sample disks represented almost 35 % of the total surface area, the gel volume change equation for a spherical geometry, was used as an approximation The diameter of the equivalent sphere was chosen so that the surface-area-to-volume ratio of the equivalent sphere was equal to that of the disk shaped sample at the start of swelling.

Figure 4.10 shows the results of fitting constant D_p, D_s and D_m to the experimental data for swelling of poly(NIPA) gel disks at 25°C. The best fit values are listed in Table 4 1. As shown in the figure, constant D_s and D_m provide fair agreement with the experimental data. The best fit D_m was close to the value of $2.2 \times 10^{-11}\ \mathrm{m}^2/\mathrm{s}$, reported by Tanaka (1985) for the poly(NIPA)-water system.

Since the experimental swelling curves were more sigmoidal than the model using constant D_m, the following two parameter forms of D_m were examined:

$$D_m = D^{\circ}\varphi_p^{\alpha} \qquad \text{(power law form)} \qquad [4.18]$$

and

$$D_m = D^{\bullet}e^{\beta(1-\varphi_p)} \qquad \text{(exponential form)} \qquad [4.19]$$

where $D^{\circ}, D^{\bullet}, \alpha$ and β are parameters whose values were obtained by fitting the theoretical curve to the experimental data. Figure 4.11 shows the best fits to the experimental data of Figure 4.10 using Equations 4.18 and 4.19. The values of the parameters are listed in Table 4.2.

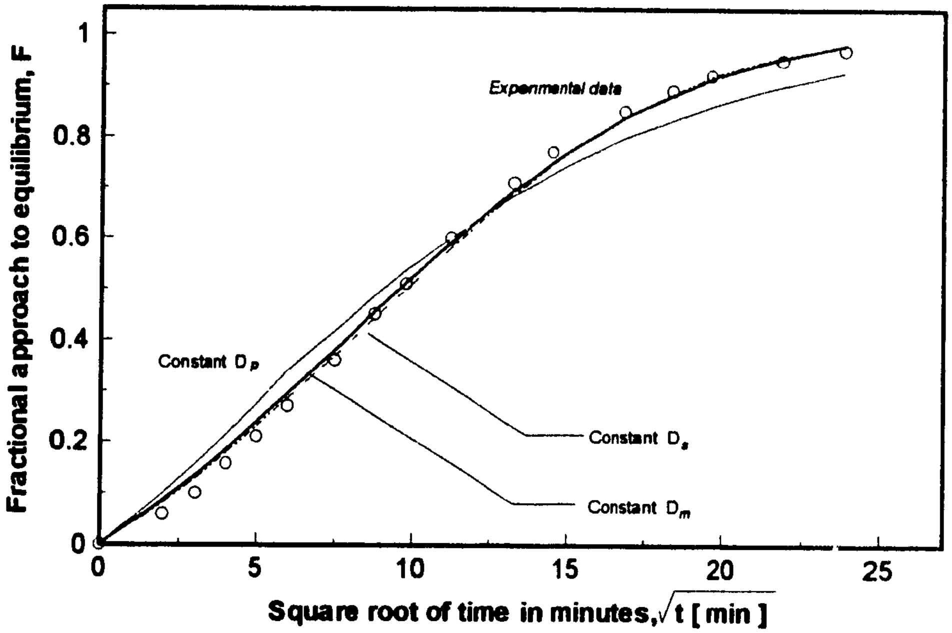

FIGURE 4.10. Best fits of model to the swelling data for poly[NIPA] disks in water at 25°C. Constant D_m (thick curve), constant D_p (thin curve) and constant D_s (dotted curve). The initial diameter and thickness were 7.5 mm and 1.08 mm, respectively [$\varphi_p^o = 0.59$, $\varphi_p^{eq} = 0.0765$, and $\Phi = 7.7$].

TABLE 4.1. Estimated values of parameters in the constant diffusion coefficients for swelling of poly (NIPA) gel disks in water :

D_p	43.5×10^{-11} m^2/s
D_s	6×10^{-11} m^2/s
D_m	5.75×10^{-11} m^2/s

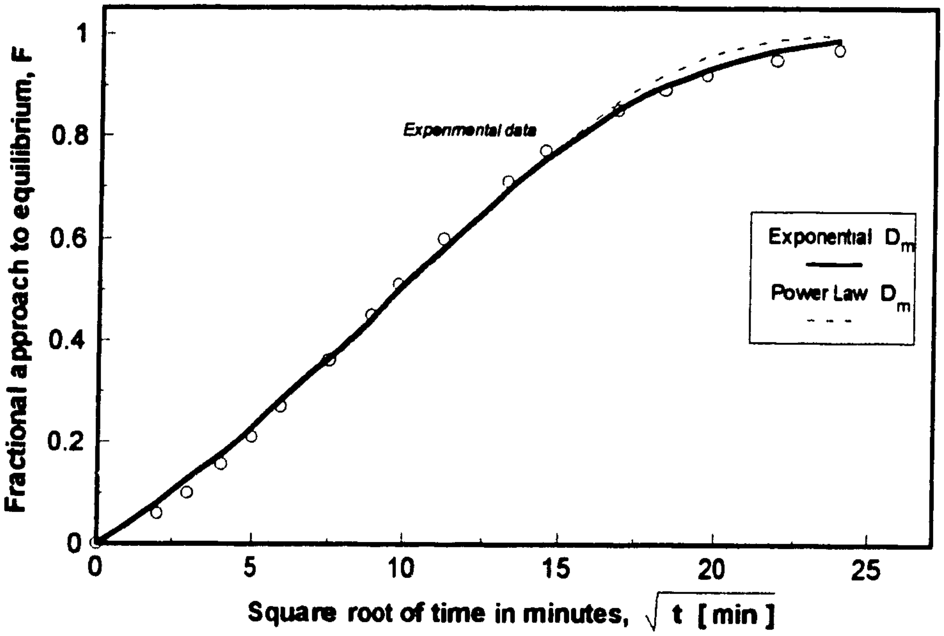

FIGURE 4.11 Best fits of model to the swelling data for poly[NIPA] disks in water at 25°C. Two different forms of composition dependent D_m as described by equations 4 18 and 4.19 were used The initial diameter and thickness were 7.5 mm and 1.08 mm, respectively [$\varphi_p^o = 0.59$, $\varphi_p^{eq} = 0.0765$, and $\Phi = 7.7$]

TABLE 4.2. Estimated values of parameters in the composition dependent diffusion coefficients for swelling of poly (NIPA) gel disks in water :

power law form	$D^{\circ} = 0.67 \times 10^{-11}$ m^2/s $\alpha = -1$
exponential form	$D^{\bullet} = 0.48 \times 10^{-11}$ m^2/s $\beta = 3$

The power law form does not fit well at the later stages of swelling, although it makes the initial portion of the swelling curve more sigmoidal than a constant D_m. The exponential fit better accounts for the swelling process throughout, but it is not a significant improvement over constant D_m. Of the representations in Equations 4.18 and 4.19, the exponential form is more reasonable because D_m remains finite as φ_p approaches zero.

A confirmation for the working hypothesis that thick disks can be represented by an equivalent sphere is provided by the following. The final equilibrium value of the surface-area-to-volume ratio of equivalent sphere was 1.2 $(\mathrm{mm})^{-1}$, as predicted by the model. This is close to the experimentally obtained value of 1.3 $(\mathrm{mm})^{-1}$ (for a fully swollen disk with thickness and diameter of 1.94 mm and 14 mm, respectively)

4.6. DIFFUSION COEFFICIENTS FROM THEORY

4.6.1 FLORY'S POLYMER GEL THEORY

Flory's *polymer gel theory* (1979) is the most widely used equation of state for non-ionic gels:

$$\mu_s - \mu_s^\circ = RT\left[\ln\left(1-\varphi_p\right) + \varphi_p + \chi\varphi_p^2 + K\left(\varphi_p^{1/3} - \tfrac{1}{2}\varphi_p\right)\right] \qquad [4.20]$$

where

μ_s = Chemical potential of the solvent in the swollen gel
μ_s° = Standard state chemical potential of the solvent
φ_p = Polymer volume fraction
R = Gas constant
T = Absolute temperature
χ = Polmer / Solvent interaction parameter
K = Parameter of gel elasticity

This equation incorporates contributions due to rubber elasticity along with the polymer-solvent affinity The expression for mutual diffusion coefficient can be written as (Vrentas *et al.*, 1986)

$$D_m = \frac{D_s^{*}\rho_p v_p \rho_s}{RT}\left(\frac{\partial \mu_s}{\partial \rho_s}\right) \qquad [4.21]$$

Using 4 20 and 4 21

$$D_m = D_s^{*}\, Q^{*} \qquad [4.22]$$

where

$$Q^{*} = \varphi_p^2\left[1 - 2\chi(1-\varphi_p) + \lambda\left(\frac{1}{\varphi_p} - 1\right)\left(\frac{1}{2} - \frac{1}{3\varphi_p^{2/3}}\right)\right] \qquad [4.23]$$

D^{*}_S is the solvent self diffusion coefficient, λ is a constant, and χ is 0.485 (Heskins *et al.*, 1968)

Figure 4 12 shows the 2 parameter (λ and D^{*}_S) fit to the data for swelling of poly (NIPA) gel disks in water at 25°C, using the above form of the mutual diffusion coefficient in the gel volume change (GVC) model The fit is poor Clearly, the Flory theory fails to provide even the qualitative form of the swelling curve.

4.6.2 SCALING THEORY

The polymer solutions have been categorized as dilute, semi-dilute or concentrated In dilute solutions the polymer coils are essentially isolated from each other, while in concentrated solutions the chains overlap extensively Semi-dilute solutions lie between these limits The range of φ_p values in this study falls in the semi-dilute region

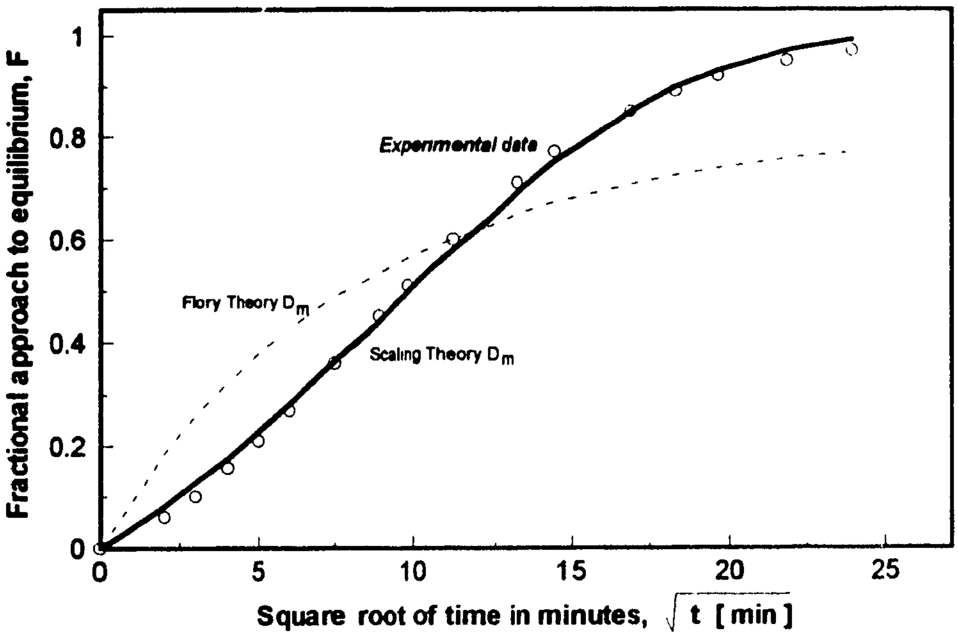

FIGURE 4.12. Fitting of the model to the same data for swelling of poly (NIPA) disks in water with D_m from Scaling and Flory theories.

One way of dealing with the diffusional transport in semi-dilute solutions is to use scaling laws. Scaling predicts the exponents in simple power laws obeyed by various polymer properties, such as the mutual diffusion coefficient, in the limit of high polymer molecular weight. However, the range of validity and the actual values of the diffusion coefficients is not predicted by scaling theories.

Weakly crosslinked, highly swollen gels are regarded as an analog of semi-dilute polymer solutions. also pictured as a transient network structure (de-Gennes, 1986). The diffusion coefficient in good solvents is given by scaling arguments as

$$D_s \propto \left(\varphi_p^{eq}\right)^{3/4} \qquad [4.24a]$$

or

$$D_m \propto \left(\varphi_p^{eq}\right)^{3/4}\left(1-\varphi_p^{eq}\right) \qquad [4.24b]$$

where, φ_p^{eq} is the polymer volume fraction at equilibrium swelling at a given temperature.

Experimentally it has been shown that D_s approaches D_c in the semi-dilute regime. Takebe *et al.* (1989) measured the cooperative diffusion coefficient for isotropically swollen polyacrylamide gels and found

$$D_c = (3.4 \pm 0.5)\times 10^{-10}\left(\varphi_p^{eq}\right)^{0.76\pm 0.03}, \quad \mathrm{m^2/s} \qquad [4.25]$$

Figure 4.12 shows the best fit to the experimental data for the swelling of poly (NIPA) disks at 25°C, using the following form of mutual diffusion coefficient

$$D_m = \lambda_1\left\{\varphi_p^{0.75} - \varphi_p^{1.75}\right\}\exp\left[\lambda_2\,\varphi_p^{\lambda_3}\left(\frac{\varphi_p^{eq}}{\varphi_p}-1\right)\right] \qquad [4.26]$$

where λ_1, λ_2 and λ_3 are parameters. This expression is consistent with Equation 4 24b because at equilibrium the exponential term vanishes The agreement between theory and data is excellent. The parameter values were 5.63×10^{-10} m^2/s , 2 45 and 0 25, respectively.

4.7. APPLICATION OF THE MODEL TO SPHERICAL HYDROGELS

The data of Tanaka *et al.*, for swelling of polyacrylamide gel beads (1979) and the collapse of poly(NIPA) gel beads (1985) in water were analyzed using the moving boundary model with constant D_m . The initial and final conditions and the best fit diffusion coefficients are given in Table 4.3

The swelling data for polyacrylamide beads are sigmoidal even for a small Φ of 1.3, as shown in Figure 4 13 However, the numerical computations for spherical geometry in Section 4 3 indicate that swelling curves are sigmoidal only for larger changes in volume (with $\Phi > 2$) The best fit to the experimental data does not have sigmoidal shape. The sigmoidal shape may have been caused by the failure of Tanaka *et al.* to remove oligomers, unreacted monomers, and other impurities by dialysis before swelling. The collapse data for poly(NIPA) beads, shown in Figure 4 14, are well predicted by a constant D_m The collapse experiments are unaffected by the oligomers etc. because these materials are removed in the initial swelling step The fitted values of D_m have an order of magnitude agreement with the values of D_m obtained from the cooperative diffusion coefficient, D_c , determined by the same authors using quasielastic light scattering or QELS

TABLE 4.3. List of information about the data used to fit the model to Tanaka *et al.* data, along with the best fit diffusion coefficients

	SWELLING	COLLAPSE
φ_p^o	0.052	0.080
φ_p^{eq}	0.040	0.094
Φ	1.3	0.85
Initial Radius (mm)	0.3130	0.2500
Final Radius (mm)	0.3388	0.2378
D_m (m^2/s) (Fitted)	4×10^{-11}	8.5×10^{-11}
D_c (m^2/s) (from QELS)	3×10^{-11}	2×10^{-11}
D_m (m^2/s) (corresponding to D_c)	2.9×10^{-11}	1.9×10^{-11}

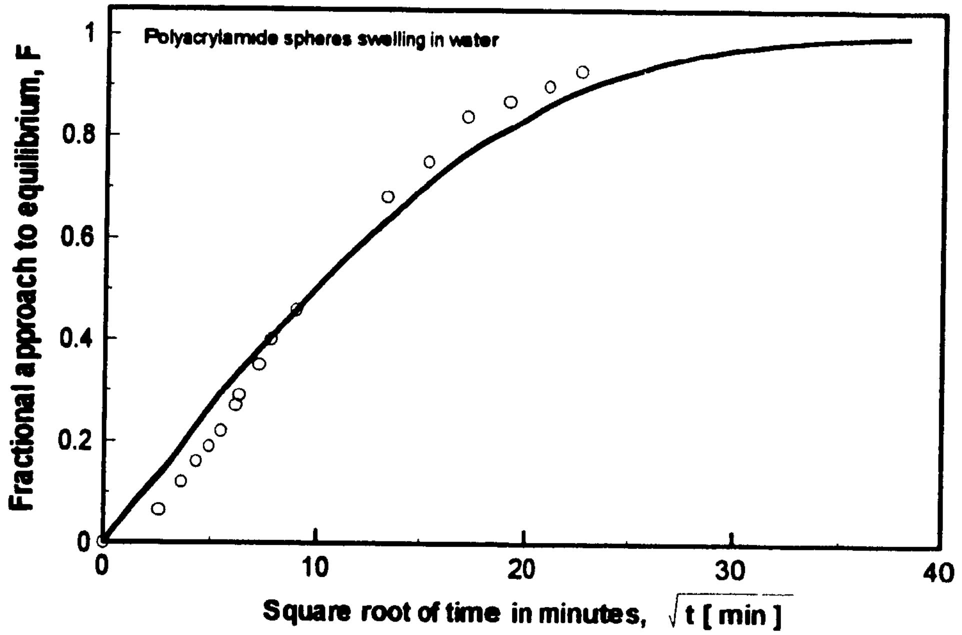

FIGURE 4.13. Best fit of the model to the data for swelling of polyacrylamide spheres in water (Tanaka et al., 1979). The parameter values and other equilibrium information are listed in Table 4.3.

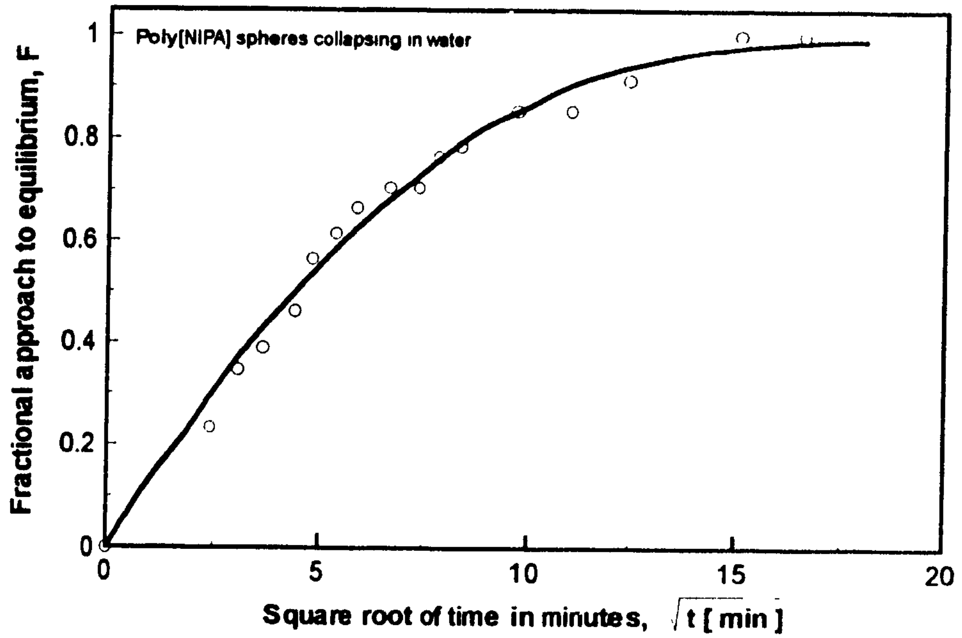

FIGURE 4.14. Best fit of the model to the data for collapse of poly (NIPA) spheres in water (Tanaka et al., 1985). The parameter values and other equilibrium information are listed in Table 4.3.

4.8. APPLICATION OF THE MODEL TO OTHER SYSTEMS

The model can be applied to any elastomer, provided it swells in a good solvent and remains rubbery during the swelling. The data of Mazich *et al* (1992) for the swelling of polyisoprene spheres in toluene were used to test the model. The swelling curve was sigmoidal for a Φ value of 6.4, in agreement with the predictions of the model with constant D_m Figure 4.15 shows best fit to the Mazich *et al.* data. The value of D_m for this fit is 1.8×10^{-10} m^2/s

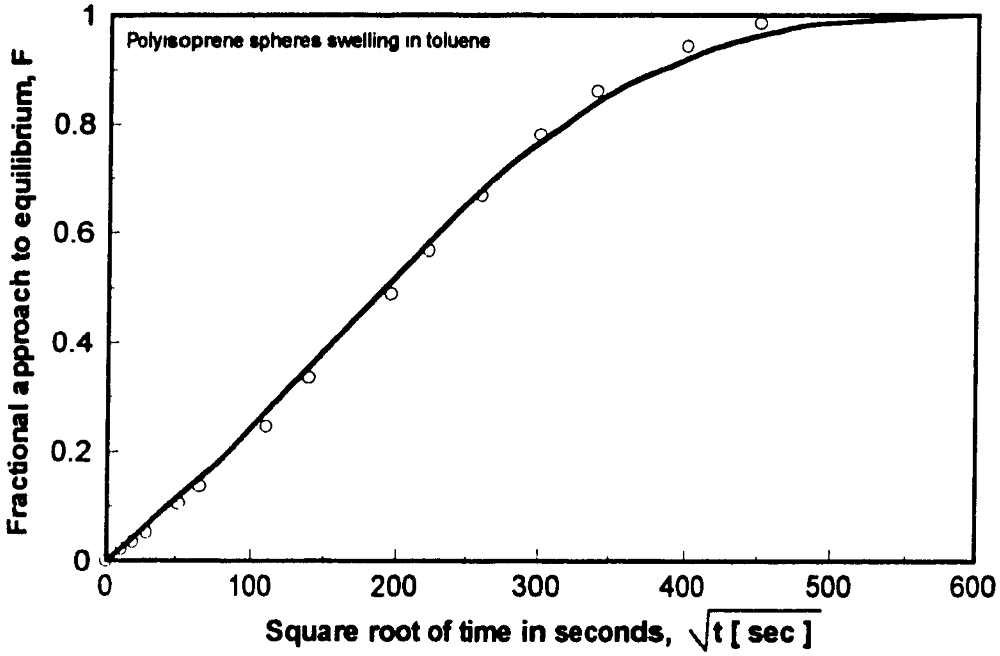

FIGURE 4.15. Swelling of polyisoprene spheres in toluene (Mazich et al., 1992). Initial radius = 6 22 mm, $\varphi_p^o = 1$, $\varphi_p^{eq} = 0.156$, and $\Phi = 6.4$. Curve: model with D_m of 1.8×10^{-10} m^2/s

4.9. DETERMINATION OF DIFFUSION TYPE FROM EXPERIMENTAL DATA

Based on the experimental and theoretical results of this study, a scheme is proposed in Figure 4.16 to determine the diffusion type from the experimental fractional approach to equilibrium curves.

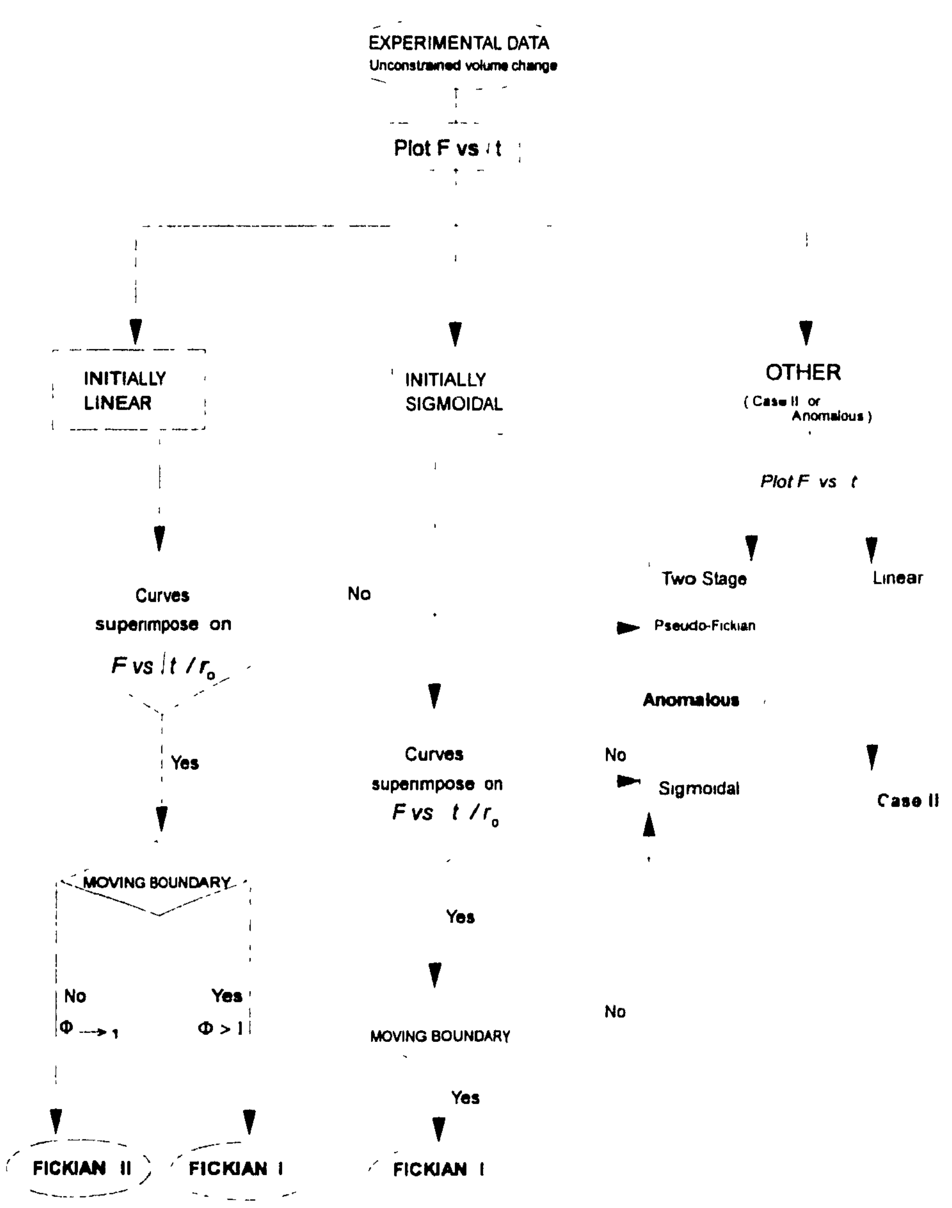

FIGURE 4.16. Proposed scheme to experimentally identify the type of diffusion

CHAPTER 5

Conclusions and Recommendations

The following conclusions and recommendations can be drawn from the work presented in this thesis

5.1. CONCLUSIONS

Non-ionic poly(NIPA) gels using different gelation temperatures, monomer concentrations, and amount of crosslinker were synthesized After collapse at 35°C, these gels undergo an appreciable change in volume when immersed in water at 25°C. About 5 minutes after immersion, the gel disks buckle, but return to a disk shape after another hour. The equilibrium swelling was isotropic. the final state of the disk-shaped samples was a swollen disk with almost same ratios of initial to final thicknesses and diameters

The maximum swelling was observed for gels with the least total monomer (%T) and crosslinker (%C) contents The collapsed and the dry gels swelled 12 and 24 times their original mass, respectively. Both %T and %C had a profound effect on the swelling equilibrium of these gels. At a fixed %T, decreasing %C by half almost doubled the equilibrium swelling ratio For a fixed % C, decreasing %T by about 40% raised the equilibrium swelling ratio by 50% In contrast, different gelation temperatures of 15°C and 25°C produced the same equilibrium swelling

The water uptake of the gels, followed a sigmoidal curve when plotted as the fractional approach to equilibrium versus the square root of time Swelling curves for different initial disk thicknesses, δ, were superimposed on plots of $\bar{F}$ vs $\sqrt{t}/\delta$. The swelling kinetics of these hydrogels are categorized as Fickian I (sigmoidal). The commonly used categorization of diffusion in polymers, as shown in Figure 2 3, does not account for any variants of Fick's first law other than Fickian II A new categorization is proposed in Figure 2.4. Diffusion is regarded as Fickian I if Fick's first law describes the diffusion flux and the boundary moves A scheme was proposed in Figure 4.16 to determine the diffusion type from experimental data

A mathematical model was formulated to describe gel volume change (GVC) under isothermal conditions. The model encompassed the general three-dimensional geometry and incorporated volume change due to swelling and the concentration dependence of diffusivity. The model assumed that diffusion was described by Fick's first law, that a polymer and solvent had constant and equal densities, and that equilibrium was attained instantaneously at the boundary For a constant D_m the fractional approach to equilibrium, F, was a function of the dimensionless time, τ_o ,and the equilibrium mass ratio, Φ

A marked difference was found between the swelling curves for disks and those for cylinders and spheres For $\Phi > 2$, the F versus $\sqrt{\tau_o}$ curves were sigmoidal for spheres and cylinders during the initial portions of swelling In contrast, the curves for disks were not sigmoidal, even for a Φ value of 100

For $\Phi = 2$, spheres swell and collapse the fastest and slabs the slowest Collapse was faster than swelling for spheres, approximately the same as swelling for cylinders, and slower than swelling for slabs

Good agreement was found between the predictions of the model and the experimental data for disk shaped poly(NIPA) gels swelling in water at 25 °C for initial and final polymer volume fractions of 0 590 and 0 076, respectively (Φ = 7 7) A sphere with a surface area to volume ratio equal to that of the disk at the start of swelling or collapse was used to represent the disk sample, since the swelling was isotropic The data were well fitted by a constant D_m. The data of Tanaka *et al.* (1979), for swelling of polyacrylamide gel beads in water, were not fitted as well with a constant D_m Collapse data, Tanaka *et al.* (1985), for poly(NIPA) gel beads in water, were well fitted with a constant D_m

The model can be applied to the swelling and collapse of any elastomer in a good solvent provided it remains rubbery, throughout. The data of Mazich *et al* (1992) for the swelling of polyisoprene spheres in toluene were well predicted with a constant D_m.

5.2. RECOMMENDATIONS

As a follow-up to this work, some pertinent areas for further research would be·

[1] Obtain collapse data for poly(NIPA) disks in water and compare with the model.

[2] Test poly(NIPA) disks with smaller equilibrium mass ratio, Φ, to examine the effect on the sigmoidal portion of the swelling curve

[3] Test undialyzed poly(NIPA) disks to examine the effect on the sigmoidal portion of the swelling curve.

[4] Investigate the swelling and collapse for poly(NIPA) spheres and cylinders in water

[5] Study the effect of the shape of different rubbery elastomers on swelling and collapse kinetics

References

Almdal, K., J Dyre, S. Hvidt, and O Kramer (1993) "Towards a Phenomenological Definition of the Term 'Gel'," *Polym. Gels and Networks*, **1**, 5

Berens, A.R and H B Hopfenberg (1978) "Diffusion and Relaxation in Glassy Polymer Powders," *Polymer*, **19**, 489.

Bird, R B , W E. Stewart, and E.N Lightfoot (1960) Transport Phenomena, Wiley, NY

Brannon-Peppas, L. and R S Harland (1990) Absorbent Polymer Technology , (Eds), Elsevier, NY

Buckley, D.J and M Berger (1962) "Swelling of Polymer Systems in Solvents II Mathematics of Diffusion," *J Polm Sci* , **56**, 175

Crank, J (1975) The Mathematics of Diffusion , Oxford University Press, London

De Gennes, P.G (1979). Scaling Concepts in Polymer Physics , Cornell University Press, Ithaca, NY

Des Cloizeaux, J (1989) "A Naive Approach to the Physics of Polymer Networks Remarks, Questions and Prospects," in Molecular Basis for Polymer Networks (Eds Baumgartner, A and C E Picot), Springer Proceedings in Physics Vol **42**, Springer-Verlag, Berlin

Fitts, D.D (1962) Nonequilibrium Thermodynamics , McGraw-Hill, NY

Flory, P J (1979) Principles of Polymer Chemistry , Cornell University Press, Ithaca, NY

Freitas, R F S and E L Cussler (1987) "Temperature Sensitive Gels as Extraction Solvents," *Chem Eng Sci* , **42**, 97

Frisch, H L (1980) "Sorption and Transport in Glassy Polymers - A Review," *Polym Eng Sci* , **20**, 2

Fujita, H (1968) "Organic vapors above the Glass Transition Temperature," in Diffusion in Polymers , (Eds Crank, J and G S Park), Acadamic Press, London

Fujita, H. (1990). Polymer Solutions , Elsevier, NY

Gehrke, S.H. (1986) Kinetics of Gel Volume Change and its Interaction with Solutes, Ph.D. Dissertation University of Minnesota, U S A

Gehrke, S H and B.G. Kabra (1991). "Synthesis of Fast Response, Temperature Sensitive Poly(N-isopropylacrylamide) Gel," *Polym. Communications*, **32**, 323

Hayes, M.J and G.S Park (1956) *Trans Faraday Soc* , **52**, 949

Heskins, M. and J.E Guillet (1968) "Solution Properties of Poly(N-isopropylacrylamide)," *J. Macromol. Sci Chem.*, **A2**, 1441

Illavský, M. (1982) "Phase Transition in Swollen Gels 2. Effect of Charge on Polyacrylamide," *Macromolecules* **15**, 782

Illavský, M., J. Hrouz, and I. Havlicek (1985) "Phase Transition in Swollen Gels 7 Effect of Charge Concentration on the Temperature Collapse of Poly(N,N-diethylacrylamide) networks in water," *Polymer*, **26**, 1514

Joshi, S and G. Astarita (1979) "Diffusion-Relaxation Coupling in Polymers which show Two-Stage Sorption Phenomena," *Polymer*, **20**, 455

Komori, T. and R. Sakamoto (1989) "On Tanaka-Fillmore's Kinetics Swelling of Gels," *Colloid Polym. Sci.*, **267**, 179

Koros, W J (Ed.) (1990). Barrier Polymers and Structures , American Chemical Society, Washington D.C.

Kudela, V. (1986). "Hydrogels," in Encyclopedia of Polymer Science and Engineering., 7, 783, Wiley-Interscience, NY.

Li, Y. and T Tanaka (1990). " Kinetics of Swelling and Shrinking of Gels," *J. Chem Phys* , **92**, 1365

Loflin, T. and E. McLaughlin (1969) "Diffusion in Binary Liquid Mixtures," *J Phy. Chem* , **73**, 186.

Mazich, K.A., G. Rossi, and C.A Smith (1992). "Kinetics of Solvent Diffusion and Swelling in a Model Elastomeric System," *Macromolecules* **25**, 6929.

Nystrom B and J Roots (1980) "Molecular Transport in Semidilute Macromolecular Solutions," *J Macromol. Sci -Rev. Macromol. Chem* , **C19**(1), 35.

Osada, Y and S B Ross-Murphy (1993). "Intelligent Gels," *Scientific American*, **268**, 82.

Peppas, N A. (Ed) (1986) Hydrogels in Medicine and Pharmacy , CRC, Boca Raton, FA.

Perez-Guerrero, A.N and L.S. Garcia-Colin (1991). "Anomalous Diffusion in Polymers. A Generalized Thermodynamic Approach," *J. Non-Equilib Thermodyn.* **16**, 201

Peters, A. and S. Candau (1986) "Kinetics of Swelling of Polyacrylamide Gels," *Macromolecules* **19**, 1952.

Press, W H , B P Flannery, S A. Tenkolsky, and W.T. Velterling (1989). Numerical Recipes in Pascal Cambridge University Press, NY.

Prud'homme, M , T H. Nguyen, and D.L. Nguyen (1989). "A Heat Transfer Analysis for Solidification of Slabs, Cylinders, and Spheres." *J. Heat Transfer* **111**, 699.

Rogers, C E (1965) "Solubility and Diffusivity," in. Physics and Chemistry of Organic Solid State (Eds Fox, D., M.M Labbes, and A Weissberger), Interscience, NY.

Rossi, G. and K.A Mazich (1991). "Kinetics of Swelling for a Cross-linked Elastomer or a Gel in the Presence of a Good Solvent." *Phys Rev A* **44**, R4743.

Rossi, G [Private Communication, February 1993]

Sparrow, E.M and W. Chuck (1984) "An Implicit/Explicit Numerical Solution Scheme for Phase-Change Problems," *Numer Heat Trans.* 7, 1

Stannet, V , H.B. Hopfenberg, and J.H. Petropoulos (1972) "Diffusion in Polymers," in MTP International Review of Science - Vol. 8 Macromolecular Science , (Ed. Brown, C.E.H), Butterworths, London.

Takebe, T, K. Nawa, S. Suehiro, and T. Hashimoto (1989). "Quasielastic Light Scattering Studies of Swollen and Stretched Polymer Gels," *J. Chem. Phys* , **91**, 4360.

Tanaka, T, L.O. Hocker, and G.B Benedek (1973). "Spectrum of Light Scattered from a Viscoelastic Gel," *J Chem. Phys.*, **59**, 5151.

Tanaka, T. and D Fillmore (1979). "Kinetics of Swelling of Gels," *J. Chem. Phys.*, **70**, 1214.

Tanaka, T. (1981). "Gels," *Scientific American*, **244**, 124

Tanaka, T., E. Sato, Y. Hirokawa, S. Hirotsu, and J. Peetermans (1985). "Critical Kinetics of Volume Phase Transition of Gels," *Phys Rev Lett* 55(22), 2455.

Tanaka, T (1986) "Gels," in Encyclopedia of Polymer Science and Engineering., 7, 517, Wiley-Interscience, NY.

Treloar, L.R.G. (1975) The Physics of Rubber Elasticity (3rd ed) , Clarendon Press, Oxford

Vasheghani-Farahani, E. (1990) Swelling and Exclusion Behaviour of Hydrogels, Ph.D Dissertation, McGill University, Montreal, Canada.

Vasheghani-Farahani, E., D.G Cooper, J H Vera, and M E Weber (1992) "Concentration of Large Biomolecules with Hydrogels," *Chem Eng Sci* , **47**, 31

Von Rosenberg, D.U. (1969). Methods of Numerical Solution of Partial Differential Equations, Elsevier, NY.

Vrentas, J S. and J L Duda (1986). " Diffusion," in Encyclopedia of Polymer Science and Engineering , 5, 36, Wiley-Interscience, NY.

Waksman, L.S , Schneider, N S and N H. Sung (1990) "Toluene Diffusion in Natural Rubber," in Barrier Polymers and Structures , (Ed. Koros, W J), American Chemical Society, Washington D.C

Appendix I

TRANSFORMATION OF EQUATION 2.27 FOR A SLAB TO MATERIAL COORDINATE FORM

For constant D_m, Equation 2.27 can be written for a slab ($i = 1$) as

$$\frac{\partial \varphi_p(r,t)}{\partial t} = D_m \, \varphi_p^2(r,t) \frac{\partial^2 \varphi_p(r,t)}{\partial r^2} \qquad [2.27a]$$

The polymer volume fraction is a function of laboratory-fixed (Eulerian) coordinate, r, and time, t

$$\varphi_p = f(r,t) \qquad [AI-1]$$

Let r be a function of the material coordinate, x, and time, t.

$$r = g(x,t) \qquad [AI-2]$$

Spatial Derivative Transformations:

The total differential of φ_p can therefore be written as

$$d\,\varphi_p = \left(\frac{\partial f}{\partial r}\right) d\,r + \left(\frac{\partial f}{\partial t}\right) d\,t \qquad [AI-3]$$

or $$\left(\frac{\partial \varphi_p}{\partial x}\right)_t = \left(\frac{\partial f}{\partial r}\right)\left(\frac{\partial g}{\partial x}\right) \qquad [AI-4]$$

or $$\left(\frac{\partial \varphi_p}{\partial t}\right)_x = \left(\frac{\partial f}{\partial r}\right)\left(\frac{\partial g}{\partial t}\right) + \left(\frac{\partial f}{\partial t}\right) \qquad [AI-5]$$

Now differentiate [AI-4]

$$\left(\frac{\partial^2 \varphi_p}{\partial x^2}\right)_t = \left(\frac{\partial f}{\partial r}\right)\left(\frac{\partial^2 g}{\partial x^2}\right) + \left(\frac{\partial f}{\partial x}\right)\left[\frac{\partial}{\partial x}\left(\frac{\partial f}{\partial r}\right)\right] \qquad [AI-6]$$

Note that

$$\frac{\partial f}{\partial r} = f^{*}(r,t) \qquad [AI\text{-}7]$$

Therefore, its total differential can be written as

$$d\left(\frac{\partial f}{\partial r}\right) = \left(\frac{\partial f^{*}}{\partial r}\right) d\,r + \left(\frac{\partial f^{*}}{\partial t}\right) d\,t \qquad [AI\text{-}8]$$

or $$\frac{\partial}{\partial x}\left(\frac{\partial f}{\partial r}\right) = \left(\frac{\partial f^{*}}{\partial r}\right)\frac{\partial g}{\partial x} = \left(\frac{\partial^2 f^{*}}{\partial r^2}\right)\frac{\partial g}{\partial x} \qquad [AI\text{-}9]$$

Substitute [AI-9] into [AI-6] to give

$$\left(\frac{\partial^2 \varphi_p}{\partial x^2}\right)_t = \left(\frac{\partial f}{\partial r}\right)\left(\frac{\partial^2 g}{\partial x^2}\right) + \left(\frac{\partial^2 f}{\partial r^2}\right)\left(\frac{\partial g}{\partial x}\right)^2 \qquad [AI\text{-}10]$$

Equation 2.27a can be written as

$$\frac{\partial f(r,t)}{\partial t} = D_m[f(r,t)]^2 \frac{\partial^2 f(r,t)}{\partial r^2} \qquad [AI\text{-}12]$$

The relationship between *r* and *x* is

$$r(x,t) = g(x,t) = \int_0^x d\beta_o \frac{1}{\varphi_p(\beta_o,t)} \qquad [AI\text{-}13]$$

where β_o is a dummy variable. From [AI-13] we obtain

$$\frac{\partial g}{\partial x} = \frac{1}{\varphi_p(x,t)} \qquad [AI\text{-}14]$$

then

$$\frac{\partial^2 g}{\partial x^2} = \frac{-1}{\left[\varphi_p(x,t)\right]^2}\left(\frac{\partial \varphi(x,t)}{\partial x}\right) \qquad [AI\text{-}15]$$

Combining [AI-4] and [AI-14]

$$\frac{\partial f}{\partial r} = \frac{1}{(\partial g/\partial x)}\left(-\frac{\partial \varphi_p}{\partial x}\right) \qquad \text{[AI-16]}$$

Combining [AI-10], [AI-14] and [AI-15]:

$$\frac{\partial^2 f}{\partial r^2} = \varphi_p^2\left[\frac{\partial^2 \varphi}{\partial x^2} + \frac{1}{\varphi_p}\left(\frac{\partial \varphi_p}{\partial x}\right)^2\right] \qquad \text{[AI-17]}$$

Time Derivative Transformation

The total derivatives of φ_p and r can be written as

$$d\,\varphi_p = \left(\frac{\partial \varphi_p}{\partial r}\right)_t d\,r + \left(\frac{\partial \varphi_p}{\partial t}\right)_r d\,t \qquad \text{[AI-18]}$$

$$dr = \left(\frac{\partial r}{\partial x}\right)_t d\,x + \left(\frac{\partial r}{\partial t}\right)_x dt \qquad \text{[AI-19]}$$

Use [AI-19] in [AI-18], to get

$$d\,\varphi_p = \left(\frac{\partial \varphi_p}{\partial r}\right)_t \left(\frac{\partial r}{\partial x}\right)_t d\,x + \left(\frac{\partial \varphi_p}{\partial r}\right)_t \left(\frac{\partial r}{\partial t}\right)_x d\,t + \left(\frac{\partial \varphi_p}{\partial t}\right)_r d\,t \qquad \text{[AI-20]}$$

or using [AI-4]

$$d\,\varphi_p = \left(\frac{\partial \varphi_p}{\partial x}\right) d\,x + \left[\left(\frac{\partial \varphi_p}{\partial r}\right)_t \left(\frac{\partial r}{\partial t}\right)_x + \left(\frac{\partial \varphi_p}{\partial t}\right)_r\right] d\,t \qquad \text{[AI-21]}$$

Since both [AI-21] and

$$d\,\varphi_p = \left(\frac{\partial \varphi_p}{\partial x}\right)_t d\,x + \left(\frac{\partial \varphi_p}{\partial t}\right)_x dt \qquad \text{[AI-22]}$$

are exact differentials, a comparison yields

$$\left(\frac{\partial \varphi_p}{\partial t}\right)_r = \left(\frac{\partial \varphi_p}{\partial t}\right)_x - \left(\frac{\partial \varphi_p}{\partial x}\right)_t \left(\frac{\partial x}{\partial r}\right)_t \left(\frac{\partial r}{\partial t}\right)_x \qquad [AI-23]$$

The polymer velocity is

$$\left(\frac{\partial r}{\partial t}\right)_x = \mathbf{u}_p \qquad [AI-24]$$

Substituting [AI-23], gives

$$\left(\frac{\partial \varphi_p}{\partial t}\right)_r = \left(\frac{\partial \varphi_p}{\partial t}\right)_x - \varphi_p \mathbf{u}_p \left(\frac{\partial \varphi_p}{\partial x}\right)_t \qquad [AI-25]$$

Use [AI-25] in conjunction with Equations 2.12, 2.13 and [AI-16], to get

$$\left(\frac{\partial \varphi_p}{\partial t}\right)_r = \left(\frac{\partial \varphi_p}{\partial t}\right)_x + D_m \varphi_p \left(\frac{\partial \varphi_p}{\partial x}\right)^2 \qquad [AI-26]$$

Substitute [AI-1], [AI-16], [AI-17] and [AI-26] into [AI-12], to get

$$\left(\frac{\partial \varphi_p}{\partial t}\right)_x = D_m \varphi_p^2 \frac{\partial^2 \varphi_p}{\partial x^2} \qquad [AI-27]$$

Appendix II

FINITE DIFFERENCE DISCRETISATION OF EQUATION 2.39

The one-dimensional gel diffusion equation in material coordinates for the planar geometry with composition dependent diffusion coefficient is

$$\frac{\partial \varphi_p}{\partial t} = \varphi_p^2 \left[D_m(\varphi_p) \frac{\partial^2 \varphi_p}{\partial x^2} + \frac{\partial D_m(\varphi_p)}{\partial \varphi_p} \left(\frac{\partial \varphi_p}{\partial x} \right)^2 \right] \qquad \text{[AII-1]}$$

This equation can be rewritten in the following form

$$\frac{\partial \varphi_p}{\partial t} = K(\varphi_p) \frac{\partial^2 \varphi_p}{\partial x^2} + K^*(\varphi_p) \left(\frac{\partial \varphi_p}{\partial x} \right)^2 \qquad \text{[AII-2]}$$

The finite difference analog of eqn [AII-2] using the Crank-Nicolson central difference scheme is.

$$\left(\frac{\varphi_{j,n+1} - \varphi_{j,n}}{\Delta t} \right) = K\left(\varphi_{j,n+1/2}\right)\left[\tfrac{1}{2}\Delta_x^2\left(\varphi_{j,n} + \varphi_{j,n+1}\right)\right] + K^*\left(\varphi_{j,n+1/2}\right)\left[\delta_x \varphi_{j,n+1/2}\right]\left[\tfrac{1}{2}\delta_x\left(\varphi_{j,n} + \varphi_{j,n+1}\right)\right]$$

[AII-3]

where $\varphi_{j,n}$ is the polymer volume fraction at grid point j ($j = 1, 2, \ldots, N+1$) at time n and

$$\delta_x \varphi_{j,n} = \left(\frac{\varphi_{j+1,n} - \varphi_{j-1,n}}{2\Delta x} \right) \qquad \text{[AII-4]}$$

$$\Delta_x^2 \varphi_{j,n} = \left(\frac{\varphi_{j+1,n} - 2\varphi_{j,n} + \varphi_{j-1,n}}{\Delta x^2} \right) \qquad \text{[AII-5]}$$

$$\varphi_{j,n+1/2} = \varphi_{j,n} + \left(\frac{\partial \varphi}{\partial t} \right)_{j,n} \left(\frac{\Delta t}{2} \right) \qquad \text{[AII-6]}$$

The resulting equations were linear algebraic equations, and were solved by the Thomas algorithm

Appendix III

SOLUTION OF THE MOVING BOUNDARY PROBLEM

For the one dimensional case, the gel diffusion equation is

$$\frac{\partial \varphi_p}{\partial t} = \frac{1}{r^{\iota}}\left[\frac{\partial}{\partial r}\left(D_m \, r^{\iota} \, \frac{\partial \varphi_p}{\partial r}\right)\right] \qquad [2.27]$$

where ι = 0, 1 and 2 for a slab, a cylinder and a sphere, respectively; r is the Eulerian spatial coordinate and t is the time. The initial and boundary conditions are given by Equations 2.28 to 2.30 and the interface equation is

$$\frac{dR}{dt} = -\frac{D_m}{\varphi_p}\frac{\partial \varphi_p}{\partial r}\bigg|_{r=R} \qquad [2.32]$$

The numerical solution was obtained using a spatial r^*, where the position of the boundary remains fixed. The coordinate r^* is defined by

$$r^* = \frac{r}{R(t)} \qquad [4.1]$$

The moving boundary is at $r^* = 1$ and the governing equations are solved within the fixed domain $0 \le r^* \le 1$.

For constant D_m, Equation 2.27 reduces to the following form.

$$\frac{\partial \varphi_p}{\partial t} = \iota \, \frac{D_m}{r}\frac{\partial \varphi_p}{\partial r} + D_m \frac{\partial^2 \varphi_p}{\partial r^2} + \frac{\partial D_m}{\partial \varphi_p}\left(\frac{\partial \varphi_p}{\partial r}\right)^2 \qquad [AIII\text{-}1]$$

Using

$$\begin{aligned} \varphi_p &= f(r,t) \\ r &= g(r^*,t) \end{aligned} \qquad [AIII\text{-}2]$$

Equation [AIII-1] is transformed to

$$\left[\frac{\partial \varphi_p}{\partial t}-\frac{r^*}{R}\frac{\partial \varphi_p}{\partial r^*}\frac{dR}{dt}\right]=\frac{1}{R^2}\left[\frac{i D_m}{r^*}\left(\frac{\partial \varphi_p}{\partial r^*}\right)+D_m\frac{\partial^2 \varphi_p}{\partial r^{*2}}+\frac{\partial D_m}{\partial \varphi_p}\left(\frac{\partial \varphi_p}{\partial r^*}\right)^2\right]$$

[AIII-3]

Further, using

$$\tau_\circ=\frac{t D_m}{R_\circ^2}$$ [4 2]

$$\varphi^*=\frac{\varphi_p^\circ-\varphi_p}{\Delta\varphi_p}$$ [4.3]

where $\Delta\varphi_p=\varphi_p^\circ-\varphi_p^{eq}$ [4.4]

Equation AIII-3 becomes

$$\frac{\partial \varphi^*}{\partial \tau_\circ}=\frac{r^*}{r^\circ}\frac{\partial \varphi^*}{\partial r^*}\frac{\partial r^\circ}{\partial \tau}+\left(\frac{1}{r^\circ}\right)^2\left[\frac{i}{r^*}\left(\frac{\partial \varphi^*}{\partial r^*}\right)+\frac{\partial^2 \varphi^*}{\partial r^{*2}}\right]$$ [4.5]

The interface equation is

$$\frac{d r^\circ}{d \tau_\circ}=\left[\Phi-1\right]\frac{1}{r^\circ}\left.\frac{\partial \varphi^*}{\partial r^*}\right|_{r^*=1}$$ [4.7]

where Φ is the equilibrium volume ratio.

The boundary and initial conditions for Equation 4.5 are

at $\tau_\circ=0$ $\quad\varphi^*=0$ $\quad$ for $\quad 0\le r^*\le 1$ [4.9a]

at $r^*=1$ $\quad\varphi^*=1$ $\quad$ for $\quad\tau_\circ>0$ [4.9b]

at $r^*=0$ $\quad\dfrac{\partial\varphi^*}{\partial r^*}=0$ $\quad$ for $\quad\tau_\circ\ge 0$ [4.9c]

The initial condition for Equation 4.7 is

$$\text{at } \tau_\circ = 0 \qquad r^\circ = 1 \tag*{[4 10]}$$

DISCRETIZATION:

The above equations were discretised using finite difference techniques with an implicit scheme for Equation 4 5 and an explicit scheme for Equation 4 7 The coupling between these equations was treated following a procedure proposed by Sparrow and Chuck (1984) The numerical approach can be summarized as follows

The second order central difference representation is used to approximate the spatial derivatives. Equation 4 5 can be readily transformed to

$$\frac{\varphi^*_{j,n+1}-\varphi^*_{j,n}}{\Delta\tau_*}=\left(\frac{1}{r^*_{n+1/2}}\right)^2\left[\frac{l}{r^*_j}\left(\frac{1}{2}\delta_x\left\{\varphi^*_{j,n+1}+\varphi^*_{j,n}\right\}\right)+\left(\frac{1}{2}\Delta^2_x\left\{\varphi^*_{j,n+1}+\varphi^*_{j,n}\right\}\right)\right]+\frac{r^*_j}{r^*_{n+1/2}}\left[\left(\frac{1}{2}\delta_x\left\{\varphi^*_{j,n+1}+\varphi^*_{j,n}\right\}\right)\right]\left(\frac{dr^*}{d\tau}\right)_{n+1/2} \tag*{[AIII-4]}$$

where

$\varphi^*_{j,n}$ is the normalised polymer volume fraction at grid point j ($j = 1, 2, \quad , N+1$) at time n

$$\delta_x\,\varphi^*_{j,n} \equiv \frac{\varphi^*_{j+1,n}-\varphi^*_{j-1,n}}{2\,\Delta r^*} \tag*{[AIII-5]}$$

$$\Delta^2_x \equiv \frac{\varphi^*_{j+1,n}-2\varphi^*_{j,n}+\varphi^*_{j-1,n}}{(\Delta r^*)^2} \tag*{[AIII-6]}$$

Starting from the discretized Equation 4 7

$$\left(\frac{dr^\circ}{d\tau_\circ}\right)_n = (\Phi-1)\frac{1}{r^\circ}\left[\frac{\varphi^*_{N+1,n}-\varphi^*_{N,n}}{\Delta r^*}\right] \tag*{[AIII-7]}$$

one obtains

$$r^\circ_{n+1/2} = r^\circ_n + \left(\frac{dr^\circ}{d\tau_\circ}\right)_n \frac{\Delta\tau_\circ}{2} \tag*{[AIII-8]}$$

to get

$$\left(\frac{dr^\circ}{d\tau_\circ}\right)_{n+1/2}=\frac{\Phi-1}{r^\circ_{n+1/2}}\left[\frac{\varphi^\bullet_{N+1,n}-\varphi^\bullet_{N,n}}{\Delta r^\bullet}\right] \qquad [\text{AIII-9}]$$

Finally the radius of the gel bead at time τ_{n+1} is calculated from

$$r^\circ_{n+1}=r^\circ_n+\left(\frac{dr^\circ}{d\tau_\circ}\right)_{n+1/2}\Delta\tau_\circ \qquad [\text{AIII-10}]$$

The Thomas algorithm for the tridiagonal matrix is used to solve the linear algebraic equations for the value of polymer volume fraction at the new time step for various nodal locations. The singularity in the first equation of the set, which exists because of the node location at $r = 0$, is handled by applying the L' hôspital's rule.

PASCAL Program

The PASCAL computer programs used to solve the above equations, are available on a diskette from Professor M E Weber[1]

---

[1] Department of Chemical Engineering, McGill University, 3480 University Street
Montréal, CANADA, H3A 2A7

Appendix IV

CONVERGENCE AND ACCURACY OF NUMERICAL COMPUTATIONS

(a) Convergence

The convergence of the computed solution for the moving boundary problem was checked with a particular emphasis on the initial portion of the swelling curve. The following tables show the numerically computed F values for spheres with a constant D_m for $\varphi_p^o = 1$, $\varphi_p^{eq} = 0.1$. Different step lengths, $1/N$, and time intervals, $\Delta\tau_o$, were used. Table A.IV.1 indicates that good convergence was achieved with 180 space increments. The largest relative deviation between F values calculated with this N and smallest $N = 200$ was 0.2 %. Table A.IV.2 gives numerical values of F for different time intervals. Convergence was satisfactory at $\Delta\tau_o = 5\times10^{6}$, with the largest relative deviation between F values at this $\Delta\tau_o$ and $\Delta\tau_o = 10^{6}$ equal to 0.4 %.

TABLE A-IV.1. Comparison of the *F* values computed for three space increments for $\Delta\tau_o = 10^{-5}$.

Dimensionless Time τ_o	*F*		
	N = 160	N = 180	N = 200
0.001	0.0233	0.0233	0.0232
0.005	0.0535	0.0533	0.0533
0.01	0.0778	0.0777	0.0776
0.05	0.1950	0.1948	0.1947
0.12	0.3287	0.3284	0.3283

TABLE A-IV.2. Comparison of *F* values computed for three time intervals for 180 space increments.

Dimensionless Time τ_o	*F*		
	$\Delta\tau_o = 10^{-5}$	$\Delta\tau_o = 5\times10^{-6}$	$\Delta\tau_o = 10^{-6}$
0.001	0.0233	0.0232	0.0231
0.005	0.0533	0.0531	0.0531
0.01	0 0777	0.0776	0.0774
0.05	0.1948	0.1944	0.1944
0.12	0.3284	0.3275	0.3275

(b) Accuracy

The value of Φ for swelling (collapse) is restricted by a minimum (maximum) limit of 1. This case corresponds to diffusion without boundary motion, hence the moving boundary solution should match the corresponding fixed boundary solution (i e. the solution of Fick's second law) as $\Phi \to 1$. This limit was used to check the accuracy of numerical computations.

The analytical solutions to Fick's second law with fixed boundary conditions are (Crank, 1975)

SLABS

$$F = 1 - \sum_{n=0}^{\infty} \frac{8}{(2n+1)^2 \pi^2} \exp\left[-(2n+1)^2 \pi^2 \tau_o\right] \qquad \text{[AIV-1]}$$

CYLINDERS

$$F = 1 - \sum_{n=1}^{\infty} \frac{4}{r_o^2 \alpha_n^2} \exp\left(-r_o^2 \alpha_n^2 \tau_o\right) \qquad \text{[AIV-2]}$$

SPHERES

$$F = 1 - \frac{6}{\pi^2}\sum_{n=1}^{\infty}\frac{1}{n^2}\exp\left(-n^2\pi^2\tau_o\right) \qquad [AIV\text{-}3]$$

Here r_o is either the half thickness for a slab, or radius of a sphere or a cylinder. The terms α_n are the positive roots of

$$J_o(\alpha_n r_o) = 0 \qquad [AIV\text{-}4]$$

where J_o is the Bessel function of the first kind of zero order, and $\alpha_n r_o$ are the zeros of that function.

The following tables show the comparison between the numerical and analytical solutions The percentage relative deviations between the analytical solution for $\Phi = 1$ and numerical solution for $\Phi = 1.01$ were less than 0.2 %.

TABLE A-IV.3. Comparison of analytical and numerical *F* values for a slab.

τ_o	*F* [SLAB]	
	$\Phi = 1$ (analytical)	$\Phi = 1.01$ (numerical)
0.001	0.0357	0.0356
0.005	0.0798	0.0796
0.01	0.1128	0.1124
0.05	0.2523	0.2518
0.1	0.3568	0.3560
0.5	0.7639	0.7635

TABLE A-IV.4. Comparison of analytical and numerical *F* values for a cylinder.

τ_o	*F* [CYLINDER]	
	$\Phi = 1$ (analytical)	$\Phi = 1.01$ (numerical)
0.001	0.0704	0.0702
0.005	0.1546	0.1539
0.01	0.2157	0.2148
0.03	0.3611	0.3600
0.05	0.4550	0.4540

TABLE A-IV.5. Comparison of analytical and numerical *F* values for a sphere.

τ_o	*F* [SPHERE]	
	$\Phi = 1$ (analytical)	$\Phi = 1.01$ (numerical)
0.0005	0.0742	0.0739
0.001	0.1040	0.1036
0.005	0.2244	0.2235
0.01	0.3085	0.3072
0.05	0.6069	0.6060
0.1	0.7705	0.7697